RCAN1 Knockout and Overexpression Recapitulate an Ensemble of Rest-activity and Circadian Disruptions Characteristic of Down Syndrome, Alzheimer's Disease, and Normative Aging

Helen Wong
University of Colorado Boulder
Jordan M. Buck
University of Colorado at Boulder: University of Colorado Boulder
Curtis Borski
University of Colorado at Boulder: University of Colorado Boulder
Jessica Pafford
University of Colorado at Boulder: University of Colorado Boulder
Bailey N. Keller
University of Colorado at Boulder: University of Colorado Boulder
Jerry A Stitzel
University of Colorado at Boulder: University of Colorado Boulder
Charles A Hoeffer (charles.hoeffer@colorado.edu)
University of Colorado Boulder https://orcid.org/0000-0002-2036-0201

Research Article

Keywords: aging, Down syndrome, Alzheimer's, calcineurin, circadian rhythms, DSCR1, free-running, light-entrained

Posted Date: November 10th, 2021

DOI: https://doi.org/10.21203/rs.3.rs-1032228/v1

Abstract

Background: *Regulator of calcineurin 1 (RCAN1)* is overexpressed in Down syndrome (DS), but RCAN1 levels are also increased in Alzheimer's disease (AD) and normal aging. AD is highly comorbid among individuals with DS and is characterized in part by progressive neurodegeneration that resembles accelerated aging. Importantly, abnormal RCAN1 levels have been demonstrated to promote memory deficits and pathophysiology symptomatic of DS, AD, and aging. Anomalous diurnal rest-activity patterns and circadian rhythm disruptions are also common in DS, AD, and aging and have been implicated in facilitating age-related cognitive decline and AD progression. However, no prior studies have assessed whether RCAN1 dysregulation may also promote the age-associated alteration of rest-activity profiles and circadian rhythms, which could in turn contribute to neurodegeneration in DS, AD, and aging.

Methods: The present study examined the impacts of RCAN1 deficiency and overexpression on the photic entrainment, circadian periodicity, intensity and distribution, diurnal patterning, and circadian rhythmicity of wheel running in young (3-6 months old) and aged (9-14 months old) mice. All data were initially analyzed by multifactorial ANOVA with variables of genotype, age, treatment, and sex considered as dependent variables.

Results: We found that daily RCAN1 levels in the hippocampi of light-entrained young mice are generally constant and that balanced RCAN1 expression is necessary for normal circadian locomotor activity rhythms. While the light-entrained diurnal period was unaltered, RCAN1-null and -overexpressing mice displayed lengthened endogenous (free-running) circadian periods like mouse models of AD and aging. In light-entrained young mice, RCAN1 knockout and overexpression also recapitulated the general hypoactivity, diurnal rest-wake pattern fragmentation, and attenuated amplitudes of circadian activity rhythms reported in DS, preclinical and clinical AD, healthily aging individuals, and rodent models thereof. Under constant darkness, RCAN1-null and -overexpressing mice displayed altered locomotor behavior indicating circadian clock dysfunction. Using the *Dp(16)1Yey/+* (*Dp16*) mouse model for DS, which expresses three copies of *Rcan1*, we found reduced wheel running activity and rhythmicity in both light-entrained and free-running young *Dp16 mice* like young RCAN1-overexpressing mice. Critically, these diurnal and circadian deficits were rescued in part or entirely by restoring *Rcan1* to two copies in *Dp16* mice.

Conclusions: Collectively, this study's findings suggest that both loss and aberrant gain of RCAN1 precipitate anomalous light-entrained diurnal and circadian activity patterns emblematic of DS, AD, and aging.

Background

Alzheimer’s disease (AD) is a progressive neurodegenerative disorder for which the predominant risk factor is age (Hebert et al., 2013). Individuals with Down syndrome (DS) are disproportionately diagnosed with the early-age onset of AD (Lott and Head, 2001), which implies that DS-associated genes may

advance AD onset reminiscent of accelerated aging. While the link between these disorders has predominantly been attributed to overexpression of amyloid precursor protein (APP) that is cleaved to yield Aβ, a defining histopathological marker of AD, considerable evidence indicates a critical contribution from *regulator of calcineurin 1* (RCAN1; also known as DSCR1). Like *APP*, *RCAN1* is a Chromosome 21 (HSA21) gene overexpressed in DS due to an extra copy (Sun et al., 2011; Wu and Song, 2013; Perluigi et al., 2014), but RCAN1 levels are also increased in the brains of sporadic AD patients (Harris et al., 2007; Sun et al., 2011; Wu and Song, 2013; Wong et al., 2015) and normally aging individuals (Cook et al., 2005; Wong et al., 2015). Therefore, RCAN1 overexpression may contribute to the early-age onset of AD-linked pathology in DS.

Consistent with a causal role for RCAN1 in the age-related progression of AD, epidemiological research reveals that the rs71324311 and rs10550296 polymorphisms of *RCAN1* lower and enhance, respectively, the risk for AD diagnosis (Lin et al., 2011). Furthermore, APP and Aβ can upregulate RCAN1 (Lloret et al., 2011; Wu et al., 2015), and RCAN1 can reciprocally induce Aβ (Wang et al., 2014) and enhance Aβ42 cytotoxicity (Lee et al., 2016). Several studies *in vitro* have demonstrated that RCAN1 overexpression mediates additional AD-like pathophysiology, including tau hyperphosphorylation, mitochondrial dysfunction, oxidative stress, synaptic defects, and neuronal apoptosis (Ma et al., 2004; Ermak et al., 2012; Wu and Song, 2013). We previously reported that neuron-specific RCAN1 overexpression in mice leads to tau pathology associated with age-dependent mitochondrial dysregulation and neurodegeneration, recapitulating hallmarks of AD (Wong et al., 2015). Interestingly, RCAN1-overexpressing (Dierssen et al., 2011; Martin et al., 2012; Bhoiwala et al., 2013; Wong et al., 2015) and RCAN1-null (Hoeffer et al., 2007) mice both exhibit AD-like synaptic plasticity and memory deficits. Likewise, overexpression and loss-of-function of the *Drosophila* RCAN1 homolog *sarah* (*sra*; also known as *nebula*) both result in learning and memory deficits (Chang et al., 2003). Taken together, these studies indicate that both upregulation and downregulation of RCAN1 may precipitate aging- and early-onset AD-associated phenotypes.

The circadian clock controls not only biological rhythms but also memory (Kondratova et al., 2010; Smarr et al., 2014; Kwapis et al., 2018) and deteriorates with age (Nakamura et al., 2011; Banks et al., 2015; Duffy et al., 2015; Wang et al., 2015), suggesting that circadian dysfunction could be a manifestation of and a risk factor for aging-associated neurodegeneration. Rest-activity fragmentation and attenuated circadian physiological and locomotor rhythms accompany normal aging, are correlated with earlier cognitive decline, and worsen with aging-related neurodegenerative diseases including AD (Satlin et al., 1995; Hatfield, 2004; Bonanni et al., 2005; Tranah et al., 2011; Lim et al., 2013; Weissová et al., 2016). Notably, rest-activity and circadian anomalies also precede the onset of cognitive deficits in AD patients and mouse models and promote pathogenic Aβ42 accumulation (Wisor et al., 2005; Ambrée et al., 2006; Musiek et al., 2018; Leng et al., 2019). Individuals with DS experience sleep-wake and rest-activity disturbances by childhood (Vicari, 2006; Ekstein et al., 2011; Bassell et al., 2015; Fernandez et al., 2017), suggesting that diurnal and circadian activity disruptions at an early age may contribute to accelerated AD onset in DS. In support of the idea that diurnal activity and circadian dysfunction drive aging-related pathogenesis, disrupting rest-activity rhythms or the circadian clock can exacerbate and elicit both aging-

(Stern and Naidoo, 2015; Yin et al., 2017; Zhao et al., 2017; Leng et al., 2019) and AD-related (Krishnan et al., 2012; Stern and Naidoo, 2015; Chauhan et al., 2017; Minakawa et al., 2017; Van Egroo et al., 2019) progressive neurodegeneration and cognitive decline. However, the molecular mechanisms underlying these age-associated diurnal and circadian alterations in DS, AD, and normal aging are poorly understood.

Considering that RCAN1 overexpression promotes AD-linked neurodegenerative phenotypes such as memory deficits in aged, but not young, mice (Wong et al., 2015), it may be that RCAN1-mediated circadian dysfunction early in the course of aging contributes to the development of cognitive impairments and AD progression. The *Drosophilia* RCAN1 ortholog *sra* regulates the circadian periodicity and rhythmicity of locomotor activity as well as the expression and post-translational modification of the circadian clock proteins PERIOD and TIMELESS (Kweon et al., 2018). Similarly, the phosphatase activity of the RCAN1 substrate calcineurin (CaN) regulates clock gene expression (Dyar et al., 2015). CaN activity also exhibits daily oscillations that mediate the expression, entrainment, and phasing of circadian rhythms such as calcium channel activity in retinal photoreceptor cells (Katz et al., 2008; Nakai et al., 2011; Huang et al., 2012; Rotter et al., 2014; Dyar et al., 2015; Kweon et al., 2018). Additionally, the RCAN1-overexpressing Ts65Dn (Stewart et al., 2007; Ruby et al., 2010), Tc1 (Heise et al., 2015), and *Dp(16)1Yey/+* (*Dp16*) (Levenga et al., 2018) mouse models for DS exhibit various abnormalities in diurnal rest-activity profiles, circadian period lengths, and amplitudes of circadian activity rhythms. Collectively, these findings implicate RCAN1 in diurnal rest-activity programs and circadian rhythmicity. Given that RCAN1 levels are elevated in the brains of DS, AD, and normally aging individuals (Wu and Song, 2013; Wong et al., 2015), aberrant RCAN1 signaling may disrupt circadian clock function and, in turn, promote cognitive decline and AD-related neurodegeneration. However, no prior studies have investigated if RCAN1 contributes to the age- and AD-related deterioration of diurnal and circadian activity rhythms.

The connections between the RCAN1 pathway, rest-activity patterns, and circadian clock function prompted us to examine diurnal and circadian activity profiles in young versus aged mice with RCAN1 overexpression and depletion. To explore the role of *RCAN1* trisomy in rest-activity and circadian abnormalities in DS, we additionally tested the hypothesis that *Rcan1* dosage correction in *Dp16* mice could restore normal diurnal rest-activity patterns or circadian activity rhythms in the DS mouse model. The present study characterizes, for the first time, the age-dependent consequences of RCAN1 dysregulation as well as the contribution of *Rcan1* triplication to DS-related impacts on periodicity of the circadian clock, photic entrainment of locomotor patterns, rest-activity profiles, and rhythmicity of circadian activity.

Materials And Methods

Animals

Rcan1 knockout (KO) mice with wild-type (WT) littermates (Vega et al., 2003) and RCAN1-overexpressing transgenic (*RCAN1* TG) mice with non-transgenic (NTG) littermates (Wong et al., 2015) were generated

and genotyped as previously described. *Dp(16)1Yey/+* (*Dp16*) mice were generated as described previously (Levenga et al., 2018) and crossed with *Rcan1*$^{(+/-)}$ mice (Vega et al., 2003) to obtain *Dp16* and WT littermates with *Dp16* mice that have *Rcan1* restored to two copies (*Dp16/Rcan1*^{2N}). All mice in this study have been backcrossed >10 generations with C57BL/6J mice to normalize the genetic background of the different mutant strains. WT mice from each respective cross are regularly used to maintain isogenic background between *Rcan1* KO, *RCAN1* TG, and *Dp16* strains. All mice were bred in the same on-site facility with ambient temperature at 20-25°C and humidity 15-65%, weaned on post-natal day (PND) 21, and provided food (Envigo Teklad 2914 irradiated rodent diet; Harlan, Madison, WI) and water *ad libitum.* With the exception of free-running experiments conducted in constant darkness (DD), all mice were maintained on a standard 12:12 h light:dark cycle (LD12:12) with lights on at 07:00 as ZT0. Wheel running experiments with the *Rcan1* KO, *Rcan1* WT, *RCAN1* TG, and NTG mice utilized between-subjects designs wherein animals were assigned to either an LD12:12 or DD regimen and tested at either PND 90-180 (young) or PND 270-420 (aged). Wheel running experiments with the *Dp16, Dp16/Rcan1*^{2N}, and WT mice utilized a within-subjects design with young (PND 90-180) mice wherein all animals were tested first in LD12:12 for two weeks and then transferred to DD for another two weeks of testing. Both sexes of each genotype were tested over multiple independent cohorts with litter-matched mice for all experiments. For each outcome measure the sample sizes for each group are indicated on the corresponding bar plots within all figure panels. All housing and experimental conditions were approved by the Institutional Animal Care and Use Committee at the University of Colorado Boulder and conformed to the *Guide for the Care and Use of Laboratory Animals* (8th Ed.) from the National Institutes of Health.

Wheel running data collection

For *Rcan1* KO, *Rcan1* WT, *RCAN1* TG, and NTG cohorts, home cage wheel running of singly-housed mice maintained in either LD12:12 or DD was wirelessly recorded in one-minute intervals for a minimum of seven (LD12:12) or ten (DD) consecutive days (between-subjects design). For *Dp16, Dp16/Rcan1*^{2N}, and WT cohorts, home cage wheel running of singly-housed mice was wirelessly recorded for fourteen consecutive days in LD12:12 followed by fourteen consecutive days in DD (within-subjects design). Home cage wheel (Cat# ENV-047, Med Associates, St. Albans, VT) revolution data were collected using Running Wheel Manager Data Acquisition Software v1.06 (Cat# SOF-861, Med Associates, St. Albans, VT). The intensity of ambient lighting for light-entrained (LD12:12) wheel running experiments was 250 lux during the light phase and zero lux during the dark phase. Free-running (DD) experiments were conducted at constant zero lux with intermittent use of dim red lamps (<1 lux) to illuminate animal care tasks in the testing room. For all datasets, the first three (*Rcan1* KO, *Rcan1* WT, *RCAN1* TG, and NTG mice) or seven (*Dp16, Dp16/Rcan1*^{2N}, and WT mice) 24-h intervals of raw wheel revolution data were excluded as the habituation period in order to mitigate the potential impacts of transients, aftereffects, acquisition time, and other experimental design-related and uncontrollable variables (Jud et al., 2005).

Notably, the between-subjects design utilized for LD12:12 and DD wheel running experiments in the *Rcan1* KO, *Rcan1* WT, RCAN1 TG, and NTG cohorts may confer potential confounds that warrant consideration when interpreting the data obtained therefrom. However, the substantial sample sizes

comprising these datasets diminish the possible impacts of any confounds stemming from the between-subjects study design. Conversely, the within-subjects design utilized for LD12:12 and DD wheel running experiments in the *Dp16*, *Dp16/Rcan1*^{2N}, and WT cohorts does not have such potential confounds. An additional limitation of the design of the present study is the differing exclusion windows utilized for processing of raw actigraphy data among *Rcan1* KO, *Rcan1* WT, *RCAN1* TG, and NTG mice relative to *Dp16*, *Dp16/Rcan1*^{2N} and WT mice. However, the wheel running phenotypes of *Dp16*, *Dp16/Rcan1*^{2N}, and WT mice when a three-day actigraphy data exclusion window is applied (data not shown) are comparable to those reported utilizing a seven-day exclusion window. These results support the validity of cross-model comparisons despite the differences in data exclusion windows utilized for actigraphic analyses of *Rcan1* KO, *Rcan1* WT, *RCAN1* TG, and NTG cohorts versus *Dp16*, *Dp16/Rcan1*^{2N}, and WT cohorts.

Periodic analyses

Analyses of the photic-entrained and circadian periodicity of wheel running were conducted as previously described (Buck et al., 2019). Briefly, to identify the fundamental period and any discrete harmonics, minute-binned raw wheel revolution data for each animal were subjected to frequency decomposition via harmonic regression at Fourier frequencies using the following equation:

$$Y(t) = A_j \sin(2\pi t/\tau_j) + e(t),\ j = 24, 12, 8, 6, 4, 3, 2, 1\ldots$$

where Y = wheel revolutions; t = time; A = amplitude (y_{max} - y_{mid}); τ = period (cycle duration, in hours); and e(t) = error term.

The zero-amplitude F-test was then applied to test the null hypothesis of zero amplitude for the fundamental period and any harmonics identified by frequency decomposition. For all (light-entrained and free-running) subjects, only the fundamental near-24-h period had significant non-zero amplitude. Fundamental period estimates were collapsed by genotype for statistical analysis.

Rhythmometric analyses

Wheel running rhythms were analyzed as previously documented (Buck et al., 2019). Summarily, wheel running rhythms were parameterized by the MESOR (oscillatory mean), amplitude (oscillatory range), and acrophase (oscillatory phase, latency to peak activity). To estimate these parameters, the fundamental period of the wheel running rhythm for each subject was incorporated into a single-component cosinor regression model defined by the following formula:

$$Y(t) = M + A\cos(2\pi/\tau + \phi) + e(t)$$

where Y = wheel revolutions; t = time; M = MESOR (y_{mid}); A = amplitude (y_{max} - y_{mid}); τ = period (cycle duration, in hours); ϕ = acrophase (value of t at y_{max}); and e(t) = error term.

This model was applied to minute-binned raw wheel revolution data, and goodness of model fit was verified by the Runs Test for each subject. The individual parameter of rhythm estimates obtained were

collapsed by genotype and, where appropriate, age for subsequent statistical analysis.

Western blot analysis

Hippocampi were dissected from young *Rcan1* WT mice (PND 90-180) maintained on an LD12:12 schedule but not provided access to running wheels to avoid potential confounds of voluntary exercise on RCAN1 expression. Tissue was collected from 6 mice of mixed sexes for each time point. Total protein extracts from the tissues were prepared for western blotting as described previously (Wong et al., 2015). Briefly, tissues were homogenized by sonication in lysis buffer containing (in mM): 10 HEPES pH 7.4, 150 NaCl, 50 NaF, 1 EDTA, 1 EGTA, and 10 $Na_4P_2O_7$ with 1X protease inhibitor cocktail III and 1X phosphatase inhibitor cocktails II and III (Sigma-Aldrich, St. Louis, MO). 20 µg of protein were then prepared in Laemmli sample buffer, resolved on 4-12% Bis-Tris gradient gels, blotted on polyvinylidene difluoride membranes, and probed with RCAN1 (Cat# D6694, Sigma-Aldrich, St. Louis, MO), brain and muscle ARNT-like factor 1 (BMAL1; Cat# sc-365645, Santa Cruz Biotechnology, Dallas, TX) and β-tubulin (Cat# ab11308, Abcam, Cambridge, MA) antibodies using standard techniques. Primary antibodies were detected with horse radish peroxidase-conjugated secondary antibodies (Promega, Madison, WI). Blots were developed by application of Enhanced Chemiluminescence substrate (GE Healthcare Life Sciences), and immunoreactive signals were acquired and densitometrically quantified as previously described (Wong et al., 2015).

Statistical Analyses

Prior to statistical analysis, all datasets were screened for outliers using the ROUT test (Q=5%), and confirmed outliers were excluded from analysis where appropriate. A maximum of three outliers were excluded per group for each dataset. All data were initially analyzed by multifactorial ANOVA to determine if there were effects of sex as a biological variable. No main effects of or interactions with sex were detected for any outcome measure; therefore, data were collapsed by sex for subsequent analysis by mixed effects ANOVA. For the *Rcan1* KO and *RCAN1* TG cohorts, genotype (*Rcan1* KO, *Rcan1* WT, *RCAN1* TG, or NTG) and age (young or aged) served as between-subjects factors while corresponding outcome measures of wheel running phenotypes served as the within-subjects factor. For *Dp16, Dp16/Rcan1*^{2N}, and WT mice, genotype served as the between-subjects factor and condition (LD12:12 or DD) and corresponding outcome measures of wheel running phenotypes served as within-subjects factors. Significant effects of and interactions among these factors were followed by Bonferroni's multiple comparisons post-hoc test. Analyses were conducted using R (https://cran.r-project.org) and SPSS 26 (IBM Analytics, Armonk, NY) and data were visualized using GraphPad Prism 8.1.1 (GraphPad Software, La Jolla, CA). For all analyses, the threshold for statistical significance (α) was set to 0.05 and adjusted for multiple comparisons.

For periodometric assessment of the *Rcan1* KO and *RCAN1* TG cohorts, the light-entrained and endogenous periodicity of wheel running were compared among young and aged *Rcan1* WT, *Rcan1* KO, NTG, and *RCAN1* TG mice by mixed ANOVA with genotype and age as between-subjects factors. For periodometric assessment of the *Dp16, Dp16/Rcan1*^{2N}, and WT mice, genotype served as the between-

subjects factor and condition (LD12:12 or DD) and outcome measure (light-entrained period length or endogenous period length) served as within-subjects factors.

For assessment of light-entrained diurnal wheel running patterns and rhythms in the *Rcan1* KO, *Rcan1* WT, *RCAN1* TG, and NTG mice, measures of mean daily wheel revolutions during the light (inactive) phase (ZT0-ZT12) and dark (active) phase (ZT12-ZT24) were compared among groups by mixed ANOVA with genotype and age as between-subjects factors and outcome measure (light phase wheel running, dark phase wheel running, or percentage of total daily wheel running occurring in the light phase) as the within-subjects factor. Parameter of rhythm estimates were compared among the groups by mixed ANOVA with the between-subjects factors genotype and age and the within-subjects factor outcome measure (MESOR, amplitude, or acrophase).

For preparatory analyses of free-running wheel running datasets in all animals, daily activity onsets were identified by linear regression to enable quantification of wheel running during the rho (inactive) phase (occurring between the offset and onset of daily activity) and the alpha (active) phase (occurring between the onset and offset of daily activity). Time intervals for free-running experiments were represented in circadian units of time (circadian hours). To calculate the duration of circadian hours for each mouse, its endogenous period length (in conventional hours) was divided by twenty-four. The average time (in circadian hours) of daily activity onset was designated circadian time (CT) 12 for each animal. Prior to rhythmometric analysis of free-running mice, minute-binned raw wheel revolution data for each subject were aligned using CT12 as the reference point.

For assessment of free-running wheel running patterns and rhythms in the *Rcan1* KO, *Rcan1* WT, *RCAN1* TG, and NTG mice, mean daily wheel revolution data for the rho and alpha phases were compared among groups by mixed ANOVA with the between-subjects factor genotype and the within-subjects factor outcome measure (total wheel running, alpha phase wheel running, rho phase wheel running, or percentage of total daily wheel running occurring in the rho phase). Parameter of rhythm estimates were analyzed by mixed ANOVA with the between-subjects factor genotype and the within-subjects factor outcome measure (MESOR, amplitude, or acrophase).

For assessment of light-entrained and free-running wheel running patterns and rhythms in *Dp16, Dp16 Rcan1*^{2N}, and WT mice, mean daily wheel revolution data for the inactive and active phases were analyzed by mixed ANOVA with the between-subjects factor genotype and the within-subjects factors condition (LD12:12 or DD) and outcome measure (total wheel running, active phase wheel running, inactive phase wheel running, or percentage of total daily wheel running occurring in the inactive phase). Parameter of rhythm estimates were analyzed by mixed ANOVA with the between-subjects factor genotype (*Dp16, Dp16 Rcan1*^{2N}, and WT) and the within-subjects factors condition (LD12:12 or DD) and outcome measure (MESOR, amplitude, or acrophase).

For western blot analysis of RCAN1 and BMAL1 content in the hippocampus of WT mice, densitometric measurements normalized by β-tubulin levels and relative to ZT11 levels were analyzed using

independent samples t-test with the between-subjects factor ZT.

Results

RCAN1 mediates the circadian periodicity but not the photic entrainment of wheel running

To probe the role of RCAN1 in age-related disruptions of circadian rhythms in DS, AD, and aging, we examined daily locomotor activity rhythms of wheel running behavior in two age groups of *Rcan1* KO mice with WT littermates and *RCAN1* TG mice with NTG littermates. In the young group, mice were tested at 3-6 months old, equivalent to early adulthood (Shoji et al., 2016) before clinical AD onset. In the aged group, mice were tested at 9-14 months old, corresponding to middle age in humans (Shoji et al., 2016) when aging-related dysfunction and preclinical AD symptoms emerge in the general population while in DS nearly all individuals have developed AD neuropathology (Lott and Head, 2001; Bishop et al., 2010; Pater, 2011; Lott, 2012). Given previous studies demonstrating that CaN (Katz et al., 2008; Dyar et al., 2015) and the *Drosophilia* RCAN1 ortholog *sra* (Nakai et al., 2011; Kweon et al., 2018) regulate the photic entrainment of circadian activity rhythms, we investigated whether RCAN1 similarly modulates light-entrained wheel running in mice. We also monitored free-running wheel activity of *Rcan1* KO and *RCAN1* TG mice in constant darkness (DD) to assess the integrity of their circadian clock and strength of their circadian rhythm.

Mean actograms of wheel-running behavior in *Rcan1* WT (Fig. 1A), *Rcan1* KO (Fig. 1B), NTG (Fig. 1C), and *RCAN1* TG (Fig. 1D) mice under LD12:12 or DD conditions revealed striking RCAN1-dependent differences in locomotor activity profiles. To quantify these differences, we first analyzed the daily periodicity of wheel running in LD12:12 or DD. We found a significant genotype x outcome measure interaction ($F_{6,307}$=2.62; p=0.017). No main effects of or interactions with age were detected, so group data were collapsed by age for further analysis. All genotypes showed a similar light-entrained period length (Fig. 1E), indicating that RCAN1 levels do not affect photic entrainment of circadian wheel running. By contrast, the endogenous period was lengthened in free-running *Rcan1* KO (p=0.041) and *RCAN1* TG (p=0.027) mice compared with *Rcan1* WT and NTG littermate controls, respectively (Fig. 1F). These data suggest that RCAN1 functions to modulate the periodicity of circadian locomotor activity rhythms.

RCAN1 knockout and overexpression alter active and inactive phase wheel running patterns in light-entrained young but not aged mice

Considering the actigraphic alterations observed in *Rcan1* KO and *RCAN1* TG mice (Fig. 1A-D), we next analyzed the intensity of light-entrained total daily wheel running (Fig. 2A) as well as daily wheel running during the dark (active) (Fig. 2B) and light (inactive) (Fig. 2C) phases. To analyze the distribution of wheel running throughout an average day, we also determined the percentage of daily wheel running during the light phase (Fig. 2D). There were significant interactions of genotype x age ($F_{3,192}$=3.22; p=0.027), age x outcome measure ($F_{2,192}$=73.09; p<1.0E-15), and genotype x age x outcome measure ($F_{6,192}$=3.38; p=0.017). In the young group, daily total wheel running was reduced both in *Rcan1* KO mice compared

with *Rcan1* WT controls (p=0.031) and in *RCAN1* TG mice compared with NTG controls (p=3.0E-4) (Fig. 2A). Furthermore, *RCAN1* TG mice exhibited reduced total daily wheel running relative to *Rcan1* KO mice (p=0.005; Fig. 2A). Across the dark and light phases, however, the wheel running patterns of *Rcan1* KO and *RCAN1* TG mice diverged. During the dark phase, both young *Rcan1* KO and *RCAN1* TG mice displayed lower daily wheel running compared with *Rcan1* WT (p=0.002) and NTG (p=0.003) controls, respectively (Fig. 2B), indicating active phase hypoactivity. During the light phase, on the other hand, young *Rcan1* KO mice were hyperactive compared with young *Rcan1* WT (p=0.023) and *RCAN1* TG (p=0.003) mice, whereas young *RCAN1* TG mice were hypoactive relative to NTG littermates (p=0.031) (Fig. 2C). Additionally, young *Rcan1* KO mice exhibited an increased percentage of total daily activity during the light phase compared with young *Rcan1* WT (p=0.011) and *RCAN1* TG (p=0.017) mice (Fig. 2D). Together these results indicate that total wheel running in an average day was reduced in both young *Rcan1 KO and RCAN1* TG mice on the LD12:12 schedule, while young *Rcan1* KO mice alone shifted wheel running normally occurring in the dark phase to the light phase.

No differences in the intensity and distribution of light-entrained wheel running were detected among the aged groups. However, consistent with the known decline in locomotor activity with age (Banks et al., 2015), aged *Rcan1* WT and NTG mice showed reduced total daily wheel running compared with young *Rcan1* WT (p=3.7E-15) and NTG (p=1.2E-10) mice, respectively (Fig. 2A). Similarly, dark phase wheel running was decreased in aged *Rcan1* WT (p=2.6E-8) and NTG (p=5.0E-6) mice compared with their respective young counterparts (Fig. 2B). Young *Rcan1* KO and *RCAN1* TG mice both showed reduced daily total wheel running (Fig. 2A) and dark phase wheel running (Fig. 2B) in the direction of aged groups, suggesting that abnormal RCAN1 levels may facilitate premature aging.

RCAN1 knockout and overexpression similarly attenuate the light-entrained diurnal rhythmicity of wheel running in young but not aged mice

Based on prior reports of reduced diurnal activity rhythm amplitudes in DS, AD, aging individuals, and animal models thereof (Satlin et al., 1995; Stewart et al., 2007; Banks et al., 2015; Heise et al., 2015; Musiek et al., 2018), each of which exhibit RCAN1 upregulation, and in *sra* KO flies, which lack the *Drosophila* homolog of RCAN1 (Kweon et al., 2018), we hypothesized that RCAN1 also regulates the rhythmicity of wheel running. Therefore, we examined the impact of RCAN1 knockout and overexpression on rhythmic characteristics of light-entrained wheel running with age. To estimate parameters of rhythm, cosinor analysis was used to curve-fit daily wheel running of young (Fig. 3A) and aged (Fig. 3B) *Rcan1* KO and *RCAN1* TG mice in LD12:12. The oscillatory mean (MESOR; Fig. 3C), range (amplitude; Fig. 3D), and phase (acrophase; Fig. 3E) of the fitted curves were estimated as measures of wheel running rhythmicity.

There were significant interactions of genotype x outcome measure ($F_{6,192}$=2.46; p=0.032), age x outcome measure ($F_{2,192}$=64.38; p=1e^{-15}), and genotype x age x outcome measure ($F_{6,192}$=3.60; p=0.016) in light-entrained circadian rhythms of wheel running. Compared with their corresponding littermate controls, young *Rcan1* KO and *RCAN1* TG mice displayed reduced MESOR (p=0.026 and p=0.010,

respectively; Fig. 3C) and amplitude (p=0.047 and p=0.028, respectively; Fig. 3D) estimates, indicating flattened circadian rhythmicity of wheel running. There were no differences among the young groups for acrophase estimates (Fig. 3E), suggesting RCAN1 does not play a role in the phasing of peak daily wheel running. No parameters of rhythm differed among aged groups (Fig. 3C-E), indicating that RCAN1 depletion and overexpression attenuate the strength of circadian locomotor rhythms in young, but not aged, mice. However, as expected, aged mice displayed dampened wheel-running rhythmicity relative to young mice, indicated by the decreased MESOR and amplitude estimates in aged versus young *Rcan1* WT (p=4.9E-11 and p=7.5E-7, respectively) and aged versus young NTG (p=1.1E-6 and p=0.004, respectively) mice. Since both MESOR and amplitude estimates were reduced in young *Rcan1* KO and *RCAN1* TG mice toward aged levels, these data further suggest that abnormal RCAN1 levels accelerate senescence phenotypes.

RCAN1 knockout and overexpression bidirectionally perturb wheel-running patterns in free-running young mice

We also assessed wheel-running profiles in the absence of light entrainment using DD (free-running) conditions. Given the altered free-running locomotor activity reported in RCAN1-overexpressing DS models (Ruby et al., 2010; Heise et al., 2015) and *sra* KO flies (Nakai et al., 2011; Kweon et al., 2018), we posited that RCAN1 additionally modulates circadian wheel-running rhythms. In support of this theory, we found RCAN1-dependent effects on the circadian period of wheel running rhythms (Fig. 1F). To determine if RCAN1 knockout and overexpression also affect the intensity and distribution of daily free-running wheel activity, we next examined total wheel running (Fig. 4A), wheel running during the alpha (active) (Fig. 4B) and rho (inactive) (Fig. 4C) phases, and the percentage of total daily wheel running during the rho phase (Fig. 4D) in free-running young *Rcan1* KO and *RCAN1* TG mice.

There was a significant genotype x outcome measure interaction ($F_{9,174}$=8.14; p=4.8e^{-9}) for daily wheel-running profiles among free-running mice. Relative to *Rcan1* WT and *RCAN1* TG mice, *Rcan1* KO mice exhibited higher total daily free-running wheel activity (p=0.008 and p=5.0E-6, respectively; Fig. 4A), resulting from increased wheel running during both the alpha (p=0.048 and p=4.0E-5, respectively; Fig. 4B) and rho (p=0.003 and p=0.009, respectively; Fig. 4C) phases. *Rcan1* KO mice also exhibited an increased percentage of total daily wheel running in the rho phase (p=0.047) compared with *Rcan1* WT controls (Fig. 4D), indicating a shift toward an increased proportion of total daily wheel running during the inactive phase. By contrast, total daily wheel activity of free-running *RCAN1* TG mice was decreased (p=0.030, Fig. 4A), largely stemming from decreased wheel running during the alpha phase (p=0.039; Fig. 4B) compared with NTG controls. Therefore, abolition of RCAN1 led to hyperactivity whereas upregulation of RCAN1 led to hypoactivity in free-running mice, suggesting that RCAN1 levels titrate circadian locomotor activity patterns in the absence of light entrainment. *RCAN1* TG mice displayed no difference in rho phase activity versus NTG controls (Fig. 4C) but trended (p=0.17) toward an increased percentage of total daily wheel running in the rho phase (Fig. 4D) like *Rcan1* KO mice. Together, these results demonstrate that RCAN1 knockout and overexpression disrupt free-running rest-activity profiles.

RCAN1 knockout and overexpression elicit divergent alterations in the circadian rhythmicity of wheel running in young mice

Considering the opposing consequences of RCAN1 deficiency and overexpression on the daily wheel running patterns of free-running young mice (Fig. 4) coupled with the RCAN1-mediated effects on diurnal rhythmicity of wheel running in light-entrained mice (Fig. 3), we postulated that RCAN1 may bidirectionally regulate the circadian rhythmicity of wheel running in young mice. To test this idea, we performed rhythmometric analysis of the wheel activity of free-running young *Rcan1* KO and *RCAN1* TG mice (Fig. 5A) to estimate the MESOR (Fig. 5B), amplitude (Fig. 5C), and acrophase (Fig. 5D) of their circadian wheel running rhythms. There was a significant genotype x outcome measure interaction ($F_{6,131}$=8.52; p=1.0E-7). Relative to *Rcan1* WT and *RCAN1* TG mice, *Rcan1* KO mice exhibited increased MESOR (p=0.008 and p=2.0E-5, respectively; Fig. 5B) and amplitude (p=0.004 and p=1.0E-6, respectively; Fig. 5C) estimates, indicating increased oscillatory means and intra-daily variability of endogenous circadian wheel running rhythms. By contrast, *RCAN1* TG mice displayed decreased MESOR (p=0.043; Fig. 5B) and amplitude (p=0.039; Fig. 5C) estimates compared with NTG controls, indicating that RCAN1 overexpression dampens the endogenous rhythmicity of daily wheel running. There were no differences in acrophase estimates among any groups (Fig. 5D), suggesting that RCAN1 levels regulate the strength and variability but not the phasing of endogenous locomotor activity rhythms. These data provide further evidence of disrupted circadian activity rhythms in young *Rcan1* KO and *RCAN1* TG mice.

Circadian periodicity and photic entrainment of wheel running are unaltered in young Dp16 mice

Given our findings of altered wheel running in young RCAN1-overexpressing mice and that *RCAN1* is triplicated in DS, we next characterized wheel running phenotypes in the *Dp16* mouse model for DS, which carries three *Rcan1* copies. To examine the specific role of RCAN1 in the DS mouse model, we also generated *Dp16* mice with *Rcan1* restored to two copies (*Dp16/Rcan1*^{2N}) and assessed whether any wheel-running alterations that *Dp16* mice exhibit could be normalized by *Rcan1* dosage correction. Because we observed that RCAN1 knockout and overexpression impacted wheel running in young mice, we compared the light-entrained (diurnal) and free-running (circadian) periodicity, patterning, and rhythmicity of wheel running among young WT, *Dp16* and *Dp16/Rcan1*^{2N} littermates. The mice underwent testing in LD12:12 conditions for two weeks, followed by constant darkness (DD) for two more weeks.

Mean actograms of wheel-running behavior revealed clear distinctions in locomotor activity profiles for WT (Fig. 6A), *Dp16* (Fig. 6B), and *Dp16/Rcan1*^{2N} (Fig. 6C) across LD12:12 and DD conditions. No main effects of or interactions among genotype, condition, or outcome measure were detected for the periodicity of wheel running. Both light-entrained diurnal and circadian period lengths (Fig. 6D) were comparable across groups. These data show that an extra copy of mouse homologs to HSA21 genes and correcting *Rcan1* dosage do not affect the periodicity of light-entrained diurnal or circadian locomotor activity rhythms in young *Dp16* mice.

Altered wheel running patterns in light-entrained and free-running young Dp16 mice are partially rescued by restoring Rcan1 to disomic levels

We next measured the intensity of total daily wheel running in young *Dp16* mice under light-entrained or free-running conditions (Fig. 7A). To analyze the distribution of wheel running throughout an average day in LD12:12 or DD, we also measured daily wheel running of young *Dp16* mice during the active (Fig. 7B) and inactive (Fig. 7C) phases separately and determined the percentage of daily wheel running occurring in the inactive phase (Fig. 7D). In contrast to the periodicity, we found interaction effects of genotype x condition ($F_{2,37}$=3.5; p=0.042), genotype x outcome measure ($F_{6,72}$=4.4; p=0.001), and condition x outcome measure ($F_{3,37}$=12.8; p=7.0E-6) on daily wheel running patterns.

Post hoc testing revealed reduced total daily wheel running in *Dp16* mice under both LD12:12 (p=5.0E-4) and DD (p=1.0E-7) conditions compared with WT mice (Fig. 7A). Critically, total daily wheel running under LD12:12 also was reduced in *Dp16* mice compared with *Dp16/Rcan1*^{2N} mice (p=0.044) while no significant difference was observed between *Dp16/Rcan1*^{2N} and WT mice (Fig. 7A). Under DD, *Dp16/Rcan1*^{2N} mice displayed total daily wheel running that was lower than in WT mice (p=0.005) but greater than in *Dp16* mice (p=0.018) (Fig. 7A). These results suggest that *Rcan1* dosage correction restores total wheel running in young *Dp16* mice at least partially to WT levels.

Similarly, during the active phases under both LD12:12 and DD conditions, *Dp16* mice showed less wheel running than WT (p=1.0E-4 and p=2.0E-7, respectively) and *Dp16/Rcan1*^{2N} (p=0.014 and p=0.015, respectively) mice (Fig. 7B). Compared with WT mice, active phase wheel running in *Dp16/Rcan1*^{2N} mice was not significantly different under LD12:12 but was reduced under DD conditions (p=0.009) (Fig. 7B). These data indicate active phase hypoactivity in both light-entrained and free-running young *Dp16* mice that are mostly rescued by restoring RCAN1 to disomic levels. No wheel running differences were detected during the inactive phase among light-entrained groups (Fig. 7C). However, during the inactive phase under DD, *Dp16* mice again showed decreased wheel running relative to WT mice (p=0.047) while no differences were detected between *Dp16/Rcan1*^{2N} and *Dp16* or WT mice (Fig. 7C). When we examined the percentage of total daily wheel running in the inactive phase, *Dp16* mice showed an increase compared with WT (p=0.041) and *Dp16/Rcan1*^{2N} (p=0.047) mice under LD12:12 but no group differences were detected under DD conditions (Fig. 7D). Together these results indicate that diurnal and circadian wheel running are reduced in *Dp16* mice, with more prominent effects during the active phase. These phenotypes were also largely dependent on *Rcan1* dosage because restoring *Rcan1* to two copies in *Dp16* mice reduced or eliminated them.

Light-entrained diurnal and circadian wheel running rhythms are diminished in young Dp16 mice and are partially normalized by restoring Rcan1 to two copies

Based on our *RCAN1* TG results (Fig. 3, 5), we hypothesized that *Rcan1* triplication in young *Dp16* mice may also impact wheel running rhythms. Therefore, we compared the characteristics of light-entrained diurnal and circadian wheel running rhythms in young WT, *Dp16*, and *Dp16/Rcan1*^{2N} mice. To this end,

we used cosinor analysis as performed earlier to curve-fit their daily wheel running under LD12:12 (Fig. 8A) and DD (Fig. 8B) conditions. The oscillatory mean (MESOR; Fig. 8C), range (amplitude; Fig. 8D), and phase (acrophase; Fig. 8E) of the fitted curves were estimated as measures of wheel running rhythmicity. Significant group x condition ($F_{2,37}$=5.0; p=0.012), group x outcome measure ($F_{4,72}$=8.9; p=7.0E-5), and condition x outcome measure ($F_{2,37}$=4.7; p=0.016) interactions were detected for daily wheel running rhythms.

Under both light entrainment and free-running conditions, *Dp16* mice exhibited decreased MESOR (p=0.003 and p=1.0E-7, respectively; Fig. 8C) and amplitude (p=7.0E-5 and p=2.0E-10, respectively; Fig. 8D) estimates compared with WT controls. These results indicate dampened wheel-running rhythmicity in young *Dp16* mice similar to young *RCAN1* TG mice (Fig. 3, 5). Consistent with the idea that RCAN1 levels regulate the oscillatory strength and range of entrained diurnal and circadian wheel running rhythms, *Dp16/Rcan1*^{2N} mice compared with *Dp16* littermates under both LD12:12 and DD exhibited increased MESOR (p=0.047 and p=0.008, respectively; Fig. 8C) and amplitude (p=0.011 and p=9.0E-5, respectively; Fig. 8D) estimates. Compared to WT littermates, no MESOR or amplitude differences were detected in *Dp16/Rcan1*^{2N} mice under LD12:12 (Fig. 8C-D), suggesting that *Rcan1* dosage correction in *Dp16* mice normalized these rhythmic characteristics. Under DD, *Dp16/Rcan1*^{2N} mice exhibited decreased MESOR (p=0.013) and amplitude (p=0.011) estimates compared with WT mice but not as severely as *Dp16* mice (Fig. 8C-D), suggesting that *Rcan1* dosage correction improved these rhythmic deficits in *Dp16* mice. As observed with young *RCAN1* TG mice (Fig. 3E, 5D), there were no differences in acrophase estimates among the groups (Fig. 8E), further suggesting that RCAN1 does not play a role in the phasing of entrained diurnal or circadian wheel-running rhythms. Because MESOR and amplitude estimates were reduced in light-entrained and free-running *Dp16* mice and restoring *Rcan1* to two copies in *Dp16* mice suppressed these effects, these data provide additional support that RCAN1 overexpression disrupts diurnal and circadian activity rhythms.

Using a heat map, we summarized the wheel running phenotypes evinced among the young cohorts of *Rcan1* KO, *RCAN1* TG, *Dp16*, and *Dp16/Rcan1*^{2N} mice (Fig. 9). This overview highlights the bidirectional influences of RCAN1 levels on wheel running phenotypes. Additionally, it intimates that restoration of RCAN1 to disomic expression levels in *Dp16/Rcan1*^{2N} mice partially normalizes aberrant wheel running phenotypes conferred by the *Dp16* genotype.

Hippocampal RCAN1 expression is normally arrhythmic in young mice

Considering the observed impacts of RCAN1 depletion and overexpression on the periodicity and rhythmicity of circadian wheel running, we sought to determine whether *Rcan1* exhibits rhythmic in the light-entrained brain. To this end, we profiled the protein abundance of RCAN1 over a 24-h period in the hippocampus, a brain region that is subject to diurnal and circadian regulation and is critically involved in both memory and biological rhythmicity (Smarr et al., 2014), domains which are impaired in DS, AD, and aging (Fernandez and Edgin, 2013; Duncan, 2019). As a reference, we also profiled the expression of the clock gene protein BMAL1 (Sangoram et al., 1998). Using western blot analysis of hippocampal tissue

collected at 6-h intervals from light-entrained young *Rcan1* WT mice (Fig. 10A), we found that levels of the larger RCAN1.1L protein isoform and the combined levels of the smaller RCAN1.1S and RCAN1.4 isoforms were stable across all time points assessed (Fig. 10B). Consistent with capturing rhythmic protein expression, we found significantly elevated BMAL1 expression at ZT23 (prior to light onset) versus ZT11 (prior to dark onset) ($t(10)=-2.277$, $p=0.046$; Fig. 10C). These results imply that RCAN1 expression is normally arrhythmic in the hippocampi of light-entrained mice during early adulthood.

Discussion

This study characterized the previously unknown impacts of RCAN1 abolition and overexpression on the entrained diurnal as well as circadian periodicity, intensity, active versus inactive phase distribution, and rhythmicity of wheel running in light-entrained and free-running young versus aged mice. Using the *Dp16* mouse model for DS, we recapitulated our findings that RCAN1 modulates light-entrained diurnal and circadian locomotor activity profiles by demonstrating *Rcan1* dosage correction improved or normalized wheel running in *Dp16* mice. We also generated novel data showing that RCAN1 expression is normally arrhythmic in the young light-entrained brain, implying that RCAN1 expression is tightly regulated to maintain constant levels throughout early adulthood. Perturbation of RCAN1 levels early during aging, as shown using young *Rcan1* KO and *RCAN1* TG mice or *Rcan1* triplication in *Dp16* mice, disrupted light-entrained diurnal as well as circadian wheel running behavior in manners reminiscent of DS, AD, and aging. Therefore, these findings demonstrate that balanced expression of RCAN1 is necessary for normal diurnal and circadian regulation of locomotor activity in mice and suggest that changes to RCAN1 levels observed in DS, AD, and normal aging (Wu and Song, 2013; Wong et al., 2015) may mediate the diurnal and circadian dysfunctions associated with these conditions (Bonanni et al., 2005; Fernandez et al., 2017; Duncan, 2019; Leng et al., 2019).

In the DS population and DS mouse models, diurnal rest-activity and circadian-related disturbances are common, but the contribution of different loci on HSA21 has been unclear. Using RCAN1-overxpressing transgenic and *Dp16* mice, we endeavored to elucidate the contribution of *RCAN1*. In light-entrained young *RCAN1* TG and *Dp16* mice, we found that daily wheel running in the dark phase was reduced and could be normalized in *Dp16* mice by restoring *Rcan1* to two copies. These data strongly suggest that RCAN1 overexpression may underlie the hypoactivity in dark-phase wheel running reported for the Tc1 mouse model of DS (Heise et al., 2015). While Tc1 mice engaged in less wheel-running activity during the dark phase, they were simultaneously more active in other locomotor behaviors, such as walking, climbing, feeding, and grooming (Heise et al., 2015). Additionally, they showed increased wheel running during the light phase (Heise et al., 2015), differing from our findings in young *RCAN1* TG and *Dp16* mice. Our data also differed from previous studies that reported hyperactivity in the Ts65Dn mouse model for DS during the dark phase (Stewart et al., 2007; Ruby et al., 2010) and hyperactivity of *Dp16* mice measured by the distance moved in the home cage during the light phase (Levenga et al., 2018). These differences from our findings may be explained by the activity measurement used (e.g., wheel running versus other locomotor behaviors) or suggest different interaction effects of the DS-related genes overexpressed in each mouse model. A hyperactive phenotype is more consistent with the hyperactivity

characteristic of DS (Vicari, 2006; Ekstein et al., 2011). However, an accelerated senescence phenotype is also characteristic of DS (Lott & Head, 2001; Lott, 2012), and general activity levels are well-known to decrease with aging (Banks et al., 2015; Musiek et al., 2018). Congruent with this, we found that decreased daily wheel running in aged mice was not further reduced by RCAN1 overexpression, suggesting that the hypoactivity in young *RCAN1* TG and *Dp16* mice reflects premature aging. RCAN1 overexpression is further implicated by the observation that *Dp16/Rcan1*^{2N} mice displayed a significant normalization of both light-entrained diurnal and circadian wheel running phenotypes compared to *Dp16* mice (Fig. 7). It remains possible that *RCAN1* TG and *Dp16* mice display hyperactivity by other measures or at earlier ages, which would be interesting to investigate in future studies.

The present study also detected attenuated rhythmicity of light-entrained diurnal wheel running as indicated by a reduced amplitude in young *RCAN1* TG and *Dp16* mice, comparable to Tc1 (Heise et al., 2015) and Ts65Dn (Stewart et al., 2007) mice. Taken together with the reduced amplitudes of diurnal rest-activity rhythms reported in DS (Fernandez et al., 2017) and the reduced impact of the DS genotype in *Dp16/Rcan1*^{2N} mice, these data suggest a primary role for RCAN1 overexpression in DS-linked dampening of diurnal activity rhythms. Consistent with premature aging in young *RCAN1* TG and *Dp16* mice, flattened rest-activity rhythmicity occurs with aging as well (Banks et al., 2015; Musiek et al., 2018). Our data also indicated reduced amplitudes of light-entrained diurnal wheel running rhythms in aged mice relative to young mice. Activity rhythm amplitudes were not further reduced in aged *RCAN1* TG mice compared with NTG littermates, suggesting RCAN1 overexpression early in life as found in DS (Sun et al., 2011; Wu and Song, 2013) accelerates the aging-associated attenuation of diurnal rest-activity rhythm amplitudes. Moreover, *RCAN1* TG mice exhibited a lengthened circadian period of wheel activity, which has similarly been observed in normally aging mice (Banks et al., 2015). This finding reveals aging-associated circadian activity rhythm dysfunction in *RCAN1* TG mice, providing additional evidence that RCAN1 overexpression promotes senescence-related phenotypes. As RCAN1 levels are elevated with age independent of DS (Cook et al., 2005; Wong et al., 2015), RCAN1 may also mediate the lengthened circadian period that manifests with normal aging. In young *Dp16* mice, interestingly, we detected no change in length of the light-entrained diurnal or circadian wheel running period whether or not RCAN1 was restored to disomic levels. This may suggest other genes triplicated in the *Dp16* model interact with RCAN1 overexpression effects to regulate diurnal and circadian rest-activity rhythms in DS. More studies testing the contribution of different loci on HSA21 to behavioral rhythm phenotypes in DS will be important. Collectively, these results suggest that RCAN1 overexpression contributes to aging-associated diurnal and circadian alterations that are accelerated in DS.

A major feature of the accelerated senescence phenotype in DS is the nearly ubiquitous early-age onset of AD, which is similarly characterized by circadian disruptions (Leng et al., 2019). Since RCAN1 is also elevated in AD (Harris et al., 2007; Sun et al., 2011; Wu and Song, 2013; Wong et al., 2015), RCAN1 overexpression may mediate DS-AD comorbidity and link diurnal rest-activity and circadian abnormalities in both disorders. Supporting this notion, the generalized hypoactivity of daily wheel running detected in young *RCAN1* TG and *Dp16* mice mimics the increased daytime sleepiness and hypoactivity documented

in AD patients (Satlin et al., 1995; Bonanni et al., 2005; Weissová et al., 2016). Furthermore, the attenuated intensity and amplitude of wheel running rhythms in young *RCAN1* TG and *Dp16* mice are analogous to the fragmentation and reduced amplitude of daily rest-activity rhythms in both preclinical (Musiek et al., 2018) and clinical (Satlin et al., 1995) AD. The lengthened circadian period of wheel running identified in young *RCAN1* TG is similarly observed in mouse models of AD (Wisor et al., 2005; Stevanovic et al., 2017). Acrophase estimates for light-entrained diurnal and circadian wheel running rhythms did not differ between young *RCAN1* TG or *Dp16* mice and WT controls, indicating that elevated RCAN1 levels do not contribute to the circadian phase shifts observed in DS, AD, aging individuals, and animal models thereof (Satlin et al., 1995; Stewart et al., 2007; Duffy et al., 2015; Fernandez et al., 2017; Duncan, 2019). In aggregate, these findings support the idea that RCAN1 overexpression mediates overlapping age-associated disturbances of light-entrained diurnal and circadian rest-activity rhythms in DS and AD.

Importantly, circadian disruptions precede the appearance of AD-linked pathology and neurodegeneration in *RCAN1* TG mice (Wong et al., 2015), mirroring the progression of disease in AD (Musiek et al., 2018; Duncan, 2019; Leng et al., 2019; Van Egroo et al., 2019). In a previous study, we found AD-like hippocampal mitochondrial dysfunction, oxidative stress, synaptic plasticity failures, and memory impairments in aged, but not young, *RCAN1* TG mice (Wong et al., 2015). However, young *RCAN1* TG mice showed AD-like increases in tau hyperphosphorylation that reached the levels of aged NTG mice. This tau hyperphosphorylation was not further increased in aged *RCAN1* TG mice (Wong et al., 2015), suggesting RCAN1 overexpression accelerates tau pathology that may feedforward and contribute to AD-like phenotypes in aged mice. In the present study, we found diurnal and circadian activity rhythm alterations reminiscent of aged phenotypes in young *RCAN1* TG mice. Thus, both tau pathology and diurnal as well as circadian rhythm dysfunction manifested before the development of other AD-related phenotypes in these mice, which models the preclinical, clinical, and pathophysiological characteristics of AD (Musiek et al., 2018; Duncan, 2019; Leng et al., 2019; Van Egroo et al., 2019). Mounting evidence points to tau pathology as a more robust biomarker of AD risk than Aβ accumulation, correlating more strongly with the onset of early cognitive symptoms and eventual clinical presentation of AD (Brier et al., 2016). Diurnal and circadian dysfunction are also emerging as risk factors for AD, based on data demonstrating that altered behavioral rhythms precede cognitive deficits in AD (Tranah et al., 2011; Lim et al., 2013; Musiek et al., 2018) and that disrupting the circadian clockwork can drive aging- and AD-related cognitive and pathological features (Yin et al., 2017; Zhao et al., 2017). Our data suggest that RCAN1 upregulation can promote or mediate the consequences of tau pathology and circadian dysfunction. Interestingly, the presence of tauopathy can disrupt biological rhythms (Stevanovic et al., 2017; Buhl et al., 2019), suggesting that RCAN1 overexpression may additively or synergistically perturb diurnal and circadian rhythmicity through upregulating tau pathology. Given the influences of biological clock function on memory performance (Smarr et al., 2014), these findings together imply that RCAN1 overexpression causes diurnal and circadian activity disruptions that may induce or exacerbate AD-related neurodegeneration.

RCAN1 deficiency also altered wheel running phenotypes in the same directions as RCAN1 overexpression for some parameters but in opposite directions for others. Neither removal nor

overexpression of RCAN1 affected the light-entrained periodicity of wheel running. However, the circadian wheel running periods in young *Rcan1* KO and *RCAN1* TG mice were comparably lengthened, indicating that optimal levels of RCAN1 are necessary to maintain the circadian periodicty of activity. With photic entrainment, RCAN1 removal and overexpression reduced daily total and dark phase wheel running and attenuated the oscillatory mean (MESOR) and oscillatory range (amplitude) of diurnal wheel running rhythms in young mice. These phenotypes resemble aging, suggesting that both loss and aberrant gain of RCAN1 may accelerate aging. In contrast to RCAN1 overexpression, RCAN1 abolition in young mice increased wheel running during the light (inactive) phase when mice are typically resting, reminiscent of increased nighttime awakenings/activity in DS and AD (Bonanni et al., 2005; Fernandez et al., 2017). Free-running *Rcan1* KO mice also showed divergent behavior from *RCAN1* TG mice. Whereas daily total and active-phase wheel running and parameters of activity rhythms including MESOR and amplitude were reduced in young *RCAN1* TG mice consistently across LD12:12 and DD conditions, these measures were increased in young free-running *Rcan1* KO mice, which differed from their light-entrained counterparts. These bidirectional effects of RCAN1 downregulation and upregulation indicate that RCAN1 titrates diurnal and circadian activity levels and rhythms, which aligns with prior studies demonstrating dose-dependent regulation of locomotor activity rhythms by the *Drosophilia* RCAN1 homolog *sra* (Kweon et al., 2018). The convergent effects of RCAN1 downregulation and upregulation on wheel running profiles also mirror previous findings that deletion of either *sra*, which disinhibited CaN activity, or *CanA-14F*, which encodes a catalytic subunit of CaN in *Drosophila*, both led to hyperactivity, short sleep, and arrhythmic clocks (Nakai et al., 2011; Kweon et al., 2018). Altogether, these data suggest that balanced RCAN1 expression is required for normative light-entrained diurnal as well as circadian activity patterns and rhythms, and deviations of RCAN1 levels confer DS-, AD-, and aging-like aberrations thereof.

Our western blot analyses revealed that RCAN1 levels are stable over a 24-h cycle in the hippocampi of young light-entrained WT mice, implying that increases to RCAN1 levels as found in *RCAN1* TG and *Dp16* mice or with aging (Wong et al., 2015) and decreases to RCAN1 levels as seen in *Rcan1* KO mice tilt the balance of RCAN1 signaling that regulates light-entrained diurnal as well as circadian functionality in early adulthood. Consistent with this result, levels of the RCAN1.1L isoform and CaN do not fluctuate in the mouse heart (Rotter et al., 2014). CaN levels in the hamster suprachiasmatic nucleus (SCN) and chick retina are similarly stable (Katz et al., 2008; Huang et al., 2012). By contrast, the RCAN1.4 isoform exhibits circadian oscillations in the mouse heart and skeletal muscle (Rotter et al., 2014; Dyar et al., 2015), demonstrating isoform-specific roles of RCAN1. Although our data suggest all RCAN1 isoforms are arrhythmic in the mouse hippocampus, it nevertheless remains feasible that fluctuations in RCAN1.4 levels are masked by RCAN1.1S or the converse, since these isoforms share the same molecular weight. Interestingly, in cases where RCAN1 or CaN levels do not show daily fluctuations, the phosphatase activity of CaN exhibits rhythmic oscillations (Katz et al., 2008; Huang et al., 2012; Rotter et al., 2014). Therefore, RCAN1 may regulate diurnal and circadian activity rhythms in part by modulating the rhythmicity of CaN activity. Since RCAN1 is known to both inhibit and facilitate CaN function (Vega et al., 2003; Liu et al., 2009; Wong et al., 2015) and to act independently of CaN (Keating et al., 2008), future studies are needed to determine how CaN participates in RCAN1-mediated daily activity rhythm

disruptions associated with DS, AD, and aging. Moreover, it will be informative to assess rhythmic changes in hippocampal CaN activity, considering that the hippocampus contains an autonomous molecular clock that has been linked to memory performance (Kondratova et al., 2010; Smarr et al., 2014; Kwapis et al., 2018), and since hippocampus-dependent memory deficits were previously observed in both *Rcan1* KO (Hoeffer et al., 2007) and *RCAN1* TG (Wong et al., 2015) mice. Furthermore, profiling the rhythmicity of RCAN1 levels and RCAN1-dependent modulation of CaN activity in other brain regions, such as the SCN, will be essential to establish if RCAN1 differentially regulates rhythmicity throughout the brain and to delineate the mechanisms whereby RCAN1 regulates diurnal and circadian activity patterns and rhythms.

Conclusions

To the best of our knowledge, the present study is the first to demonstrate that both abolition and amplification of RCAN1 expression elicit an ensemble of DS-, AD-, and aging-like alterations in the diurnal and circadian patterns, periodicities, and rhythmicities of locomotion in young mice. Based on these novel findings, we posit that changes to RCAN1 levels in the brain throughout aging perturb light-entrained diurnal and circadian activity, which in turn contributes to age-related cognitive impairments and AD progression. Accordingly, RCAN1 overexpression beginning during development in DS may mediate the early appearance of circadian activity disturbances and accelerated onset of AD- and aging-like neurodegeneration in the DS population. In sporadic AD, RCAN1 upregulation may contribute to diurnal and circadian rest-activity rhythm anomalies that both promote and are exacerbated by AD pathology. More generally, perturbation of rest-activity profiles stemming from increased RCAN1 levels in normatively aging individuals may mediate aging-associated cognitive decline. Future research is warranted to determine whether pharmacological targeting of RCAN1, either alone or in combination with light or melatonin therapy, may be an effective treatment for DS, AD, or aging-related phenotypes.

List Of Abbreviations

Down syndrome (DS) Alzheimer’s disease (AD) Regulator of Calcineurin1 (RCAN1)

Calcineurin (CaN) rhythm-adjusted mean (MESOR) suprachiasmatic nucleus (SCN)

Declarations

Ethics Statement All procedures were approved by the University of Colorado, Boulder Institutional Animal Care and Use Committee and conformed to the National Institutes of Health’s Guide for the Care and Use of Laboratory Animals.

Consent for publication Not applicable

Availability of Data and Materials The datasets used and/or analysed during the current study are available from the corresponding author on reasonable request

Competing Interests The authors declare that they have no competing interests

Funding Research support was provided by the National Institutes of Health (R01 NS086933-01, T32 DA017637, and T32 MH016880), Linda Crnic Institute, LeJeune Foundation, and Alzheimer's Association (MNIRGDP-12-258900).

Author Contributions HW and CAH designed the experiments. HW, CB, JTP, and BNK performed the experiments. JMB analyzed the data. HW and JMB wrote the manuscript with input from JAS and CAH.

Acknowledgements We thank Jarryd Butler, Lauren LaPlante, Caleb Anderson, Kevin Jones, and Andrew Cooper-Sansone for assistance with genotyping, running wheel experiments, and sharing mouse reagents.

References

1. Ambrée, O., Touma, C., Görtz, N., Keyvani, K., Paulus, W., Palme, R., et al. (2006). Activity changes and marked stereotypic behavior precede Abeta pathology in TgCRND8 Alzheimer mice. *Neurobiol. Aging* 27, 955–964. doi:10.1016/j.neurobiolaging.2005.05.009.
2. Banks, G., Heise, I., Starbuck, B., Osborne, T., Wisby, L., Potter, P., et al. (2015). Genetic background influences age-related decline in visual and nonvisual retinal responses, circadian rhythms, and sleep. *Neurobiology of Aging* 36, 380–393. doi:10.1016/j.neurobiolaging.2014.07.040.
3. Bassell, J. L., Phan, H., Leu, R., Kronk, R., and Visootsak, J. (2015). Sleep profiles in children with down syndrome. *Am. J. Med. Genet.* 167, 1830–1835. doi:10.1002/ajmg.a.37096.
4. Bhoiwala, D. L., Koleilat, I., Qian, J., Beyer, B., Hushmendy, S. F., Mathew, A., et al. (2013). Overexpression of RCAN1 isoform 4 in mouse neurons leads to a moderate behavioral impairment. *Neurological Research* 35, 79–89. doi:10.1179/1743132812Y.0000000117.
5. Bishop, N. A., Lu, T., and Yankner, B. A. (2010). Neural mechanisms of ageing and cognitive decline. *Nature* 464, 529–535. doi:10.1038/nature08983.
6. Bonanni, E., Maestri, M., Tognoni, G., Fabbrini, M., Nucciarone, B., Manca, M. L., et al. (2005). Daytime sleepiness in mild and moderate Alzheimer's disease and its relationship with cognitive impairment. *Journal of Sleep Research* 14, 311–317. doi:10.1111/j.1365-2869.2005.00462.x.
7. Brier, M. R., Gordon, B., Friedrichsen, K., McCarthy, J., Stern, A., Christensen, J., et al. (2016). Tau and Ab imaging, CSF measures, and cognition in Alzheimer's disease. *Science Translational Medicine* 8, 10.
8. Buck, J. M., Sanders, K. N., Wageman, C. R., Knopik, V. S., Stitzel, J. A., and O'Neill, H. C. (2019). Developmental nicotine exposure precipitates multigenerational maternal transmission of nicotine preference and ADHD-like behavioral, rhythmometric, neuropharmacological, and epigenetic anomalies in adolescent mice. *Neuropharmacology* 149, 66–82. doi:10.1016/j.neuropharm.2019.02.006.

9. Buhl, E., Higham, J. P., and Hodge, J. J. L. (2019). Alzheimer's disease-associated tau alters Drosophila circadian activity, sleep and clock neuron electrophysiology. *Neurobiology of Disease* 130, 104507. doi:10.1016/j.nbd.2019.104507.
10. Chang, K. T., Shi, Y.-J., and Min, K.-T. (2003). The Drosophila homolog of Down's syndrome critical region 1 gene regulates learning: Implications for mental retardation. *Proceedings of the National Academy of Sciences* 100, 15794–15799. doi:10.1073/pnas.2536696100.
11. Chauhan, R., Chen, K.-F., Kent, B. A., and Crowther, D. C. (2017). Central and peripheral circadian clocks and their role in Alzheimer's disease. *Dis. Model. Mech.* 10, 1187–1199. doi:10.1242/dmm.030627.
12. Cook, C. N., Hejna, M. J., Magnuson, D. J., and Lee, J. M. (2005). Expression of calcipressin1, an inhibitor of the phosphatase calcineurin, is altered with aging and Alzheimer's disease. *JAD* 8, 63–73. doi:10.3233/JAD-2005-8108.
13. Dierssen, M., Arqué, G., McDonald, J., Andreu, N., Martínez-Cué, C., Flórez, J., et al. (2011). Behavioral characterization of a mouse model overexpressing DSCR1/ RCAN1. *PLoS ONE* 6, e17010. doi:10.1371/journal.pone.0017010.
14. Duffy, J. F., Zitting, K.-M., and Chinoy, E. D. (2015). Aging and Circadian Rhythms. *Sleep Medicine Clinics* 10, 423–434. doi:10.1016/j.jsmc.2015.08.002.
15. Duncan, M. J. (2019). Interacting influences of aging and Alzheimer's disease on circadian rhythms. *Eur J Neurosci*. doi:10.1111/ejn.14358.
16. Dyar, K. A., Ciciliot, S., Tagliazucchi, G. M., Pallafacchina, G., Tothova, J., Argentini, C., et al. (2015). The calcineurin-NFAT pathway controls activity-dependent circadian gene expression in slow skeletal muscle. *Molecular Metabolism* 4, 823–833. doi:10.1016/j.molmet.2015.09.004.
17. Ekstein, S., Glick, B., Weill, M., Kay, B., and Berger, I. (2011). Down syndrome and attention-deficit/hyperactivity disorder (ADHD). *J Child Neurol* 26, 1290–1295. doi:10.1177/0883073811405201.
18. Ermak, G., Sojitra, S., Yin, F., Cadenas, E., Cuervo, A. M., and Davies, K. J. A. (2012). Chronic expression of RCAN1-1L protein induces mitochondrial autophagy and metabolic shift from oxidative phosphorylation to glycolysis in neuronal cells. *J. Biol. Chem.* 287, 14088–14098. doi:10.1074/jbc.M111.305342.
19. Fernandez, F., and Edgin, J. O. (2013). Poor sleep as a precursor to cognitive decline in Down syndrome: a hypothesis. *J Alzheimers Dis Parkinsonism* 03. doi:10.4172/2161-0460.1000124.
20. Fernandez, F., Nyhuis, C. C., Anand, P., Demara, B. I., Ruby, N. F., Spanò, G., et al. (2017). Young children with Down syndrome show normal development of circadian rhythms, but poor sleep efficiency: a cross-sectional study across the first 60 months of life. *Sleep Medicine* 33, 134–144. doi:10.1016/j.sleep.2016.12.026.
21. Frontiers RCAN1 Manuscript 4-18-21.docx.
22. Harris, C. D., Ermak, G., and Davies, K. J. A. (2007). RCAN1-1L is overexpressed in neurons of Alzheimer's disease patients. *FEBS Journal* 274, 1715–1724. doi:10.1111/j.1742-

4658.2007.05717.x.

23. Hatfield, C. F. (2004). Disrupted daily activity/rest cycles in relation to daily cortisol rhythms of home-dwelling patients with early Alzheimer's dementia. *Brain* 127, 1061–1074. doi:10.1093/brain/awh129.
24. Hebert, L. E., Weuve, J., Scherr, P. A., and Evans, D. A. (2013). Alzheimer disease in the United States (2010-2050) estimated using the 2010 census. *Neurology* 80, 1778–1783. doi:10.1212/WNL.0b013e31828726f5.
25. Heise, I., Fisher, S. P., Banks, G. T., Wells, S., Peirson, S. N., Foster, R. G., et al. (2015). Sleep-like behavior and 24-h rhythm disruption in the Tc1 mouse model of Down syndrome: Sleep and rhythm disruption in Tc1 mice. *Genes, Brain and Behavior* 14, 209–216. doi:10.1111/gbb.12198.
26. Hoeffer, C. A., Dey, A., Sachan, N., Wong, H., Patterson, R. J., Shelton, J. M., et al. (2007). The Down Syndrome Critical Region protein RCAN1 regulates long-term potentiation and memory via inhibition of phosphatase signaling. *Journal of Neuroscience* 27, 13161–13172. doi:10.1523/JNEUROSCI.3974-07.2007.
27. Huang, C. C.-Y., Ko, M. L., Vernikovskaya, D. I., and Ko, G. Y.-P. (2012). Calcineurin serves in the circadian output pathway to regulate the daily rhythm of L-type voltage-gated calcium channels in the retina. *J. Cell. Biochem.* 113, 911–922. doi:10.1002/jcb.23419.
28. Jud, C., Schmutz, I., Hampp, G., Oster, H., and Albrecht, U. (2005). A guideline for analyzing circadian wheel-running behavior in rodents under different lighting conditions. *Biol. Proced. Online* 7, 101–116. doi:10.1251/bpo109.
29. Katz, M., Simonetta, S., Ralph, M., and Golombek, D. (2008). Immunosuppressant calcineurin inhibitors phase shift circadian rhythms and inhibit circadian responses to light. *Pharmacology Biochemistry and Behavior* 90, 763–768. doi:10.1016/j.pbb.2008.05.017.
30. Keating, D. J., Dubach, D., Zanin, M. P., Yu, Y., Martin, K., Zhao, Y.-F., et al. (2008). DSCR1/RCAN1 regulates vesicle exocytosis and fusion pore kinetics: implications for Down syndrome and Alzheimer's disease. *Human Molecular Genetics* 17, 1020–1030. doi:10.1093/hmg/ddm374.
31. Kondratova, A. A., Dubrovsky, Y. V., Antoch, M. P., and Kondratov, R. V. (2010). Circadian clock proteins control adaptation to novel environment and memory formation. *aging* 2, 285–297. doi:10.18632/aging.100142.
32. Krishnan, N., Rakshit, K., Chow, E. S., Wentzell, J. S., Kretzschmar, D., and Giebultowicz, J. M. (2012). Loss of circadian clock accelerates aging in neurodegeneration-prone mutants. *Neurobiology of Disease* 45, 1129–1135. doi:10.1016/j.nbd.2011.12.034.
33. Kwapis, J. L., Alaghband, Y., Kramár, E. A., López, A. J., Vogel Ciernia, A., White, A. O., et al. (2018). Epigenetic regulation of the circadian gene Per1 contributes to age-related changes in hippocampal memory. *Nat Commun* 9, 3323. doi:10.1038/s41467-018-05868-0.
34. Kweon, S. H., Lee, J., Lim, C., and Choe, J. (2018). High-amplitude circadian rhythms in *Drosophila* driven by calcineurin-mediated post-translational control of *sarah*. *Genetics*, genetics.300808.2018. doi:10.1534/genetics.118.300808.

35. Lee, S., Bang, S. M., Hong, Y. K., Lee, J. H., Jeong, H., Park, S. H., et al. (2016). The calcineurin inhibitor Sarah (Nebula) exacerbates Aβ42 phenotypes in a *Drosophila* model of Alzheimer's disease. *Dis. Model. Mech.* 9, 295–306. doi:10.1242/dmm.018069.
36. Leng, Y., Musiek, E. S., Hu, K., Cappuccio, F. P., and Yaffe, K. (2019). Association between circadian rhythms and neurodegenerative diseases. *Lancet Neurol* 18, 307–318. doi:10.1016/S1474-4422(18)30461-7.
37. Levenga, J., Peterson, D. J., Cain, P., and Hoeffer, C. A. (2018). Sleep behavior and EEG oscillations in aged Dp(16)1Yey/+ mice: a Down syndrome model. *Neuroscience* 376, 117–126. doi:10.1016/j.neuroscience.2018.02.009.
38. Lim, A. S. P., Kowgier, M., Yu, L., Buchman, A. S., and Bennett, D. A. (2013). Sleep Fragmentation and the Risk of Incident Alzheimer's Disease and Cognitive Decline in Older Persons. *Sleep* 36, 1027–1032. doi:10.5665/sleep.2802.
39. Lin, K., Tang, M., Guo, Y., Han, H., and Lin, Y. (2011). Two polymorphisms of RCAN1 gene associated with Alzheimer's disease in the Chinese Han population. *East Asian Archives of Psychiatry* 21, 79–84.
40. Liu, Q., Busby, J. C., and Molkentin, J. D. (2009). Interaction between TAK1–TAB1–TAB2 and RCAN1–calcineurin defines a signalling nodal control point. *Nat Cell Biol* 11, 154–161. doi:10.1038/ncb1823.
41. Lloret, A., Badia, M.-C., Giraldo, E., Ermak, G., Alonso, M.-D., Pallardó, F. V., et al. (2011). Amyloid-β toxicity and tau hyperphosphorylation are linked via RCAN1 in Alzheimer's disease. *JAD* 27, 701–709. doi:10.3233/JAD-2011-110890.
42. Lott, I. T. (2012). Neurological phenotypes for Down syndrome across the life span. *Prog Brain Res* 197, 101–121. doi:10.1016/B978-0-444-54299-1.00006-6.
43. Lott, I. T., and Head, E. (2001). Down syndrome and Alzheimer's disease: a link between development and aging. *Ment Retard Dev Disabil Res Rev* 7, 172–178. doi:10.1002/mrdd.1025.
44. Ma, H., Xiong, H., Liu, T., Zhang, L., Godzik, A., and Zhang, Z. (2004). Aggregate formation and synaptic abnormality induced by DSCR1. *Journal of Neurochemistry* 88, 1485–1496. doi:10.1046/j.1471-4159.2003.02294.x.
45. Martin, K. R., Corlett, A., Dubach, D., Mustafa, T., Coleman, H. A., Parkington, H. C., et al. (2012). Over-expression of RCAN1 causes Down syndrome-like hippocampal deficits that alter learning and memory. *Human Molecular Genetics* 21, 3025–3041. doi:10.1093/hmg/dds134.
46. Minakawa, E. N., Miyazaki, K., Maruo, K., Yagihara, H., Fujita, H., Wada, K., et al. (2017). Chronic sleep fragmentation exacerbates amyloid β deposition in Alzheimer's disease model mice. *Neurosci. Lett.* 653, 362–369. doi:10.1016/j.neulet.2017.05.054.
47. Musiek, E. S., Bhimasani, M., Zangrilli, M. A., Morris, J. C., Holtzman, D. M., and Ju, Y.-E. S. (2018). Circadian rest-activity pattern changes in aging and preclinical Alzheimer disease. *JAMA Neurol* 75, 582. doi:10.1001/jamaneurol.2017.4719.

48. Nakai, Y., Horiuchi, J., Tsuda, M., Takeo, S., Akahori, S., Matsuo, T., et al. (2011). Calcineurin and its regulator Sra/DSCR1 are essential for sleep in Drosophila. *Journal of Neuroscience* 31, 12759–12766. doi:10.1523/JNEUROSCI.1337-11.2011.

49. Nakamura, T. J., Nakamura, W., Yamazaki, S., Kudo, T., Cutler, T., Colwell, C. S., et al. (2011). Age-Related Decline in Circadian Output. *Journal of Neuroscience* 31, 10201–10205. doi:10.1523/JNEUROSCI.0451-11.2011.

50. Pater, C. (2011). Mild cognitive impairment (MCI) - the novel trend of targeting Alzheimer's disease in its early stages - methodological considerations. *Curr Alzheimer Res* 8, 798–807.

51. Perluigi, M., Pupo, G., Tramutola, A., Cini, C., Coccia, R., Barone, E., et al. (2014). Neuropathological role of PI3K/Akt/mTOR axis in Down syndrome brain. *Biochimica et Biophysica Acta (BBA) - Molecular Basis of Disease* 1842, 1144–1153. doi:10.1016/j.bbadis.2014.04.007.

52. Rotter, D., Grinsfelder, D. B., Parra, V., Pedrozo, Z., Singh, S., Sachan, N., et al. (2014). Calcineurin and its regulator, RCAN1, confer time-of-day changes in susceptibility of the heart to ischemia/reperfusion. *Journal of Molecular and Cellular Cardiology* 74, 103–111. doi:10.1016/j.yjmcc.2014.05.004.

53. Ruby, N. F., Fernandez, F., Zhang, P., Klima, J., Heller, H. C., and Garner, C. C. (2010). Circadian locomotor rhythms are normal in Ts65Dn "Down Syndrome" mice and unaffected by pentylenetetrazole. *J Biol Rhythms* 25, 63–66. doi:10.1177/0748730409356202.

54. Sangoram, A. M., Saez, L., Antoch, M. P., Gekakis, N., Staknis, D., Whiteley, A., et al. (1998). Mammalian circadian autoregulatory loop: a timeless ortholog and mPer1 interact and negatively regulate CLOCK-BMAL1-induced transcription. *Neuron* 21, 1101–1113. doi:10.1016/s0896-6273(00)80627-3.

55. Satlin, A., Volicer, L., Stopa, E. G., and Harper, D. (1995). Circadian locomotor activity and core-body temperature rhythms in Alzheimer's disease. *Neurobiol. Aging* 16, 765–771.

56. Shoji, H., Takao, K., Hattori, S., and Miyakawa, T. (2016). Age-related changes in behavior in C57BL/6J mice from young adulthood to middle age. *Mol Brain* 9, 11. doi:10.1186/s13041-016-0191-9.

57. Smarr, B. L., Jennings, K. J., Driscoll, J. R., and Kriegsfeld, L. J. (2014). A time to remember: the role of circadian clocks in learning and memory. *Behav Neurosci* 128, 283–303. doi:10.1037/a0035963.

58. Stern, A. L., and Naidoo, N. (2015). Wake-active neurons across aging and neurodegeneration: a potential role for sleep disturbances in promoting disease. *SpringerPlus* 4, 25. doi:10.1186/s40064-014-0777-6.

59. Stevanovic, K., Yunus, A., Joly-Amado, A., Gordon, M., Morgan, D., Gulick, D., et al. (2017). Disruption of normal circadian clock function in a mouse model of tauopathy. *Experimental Neurology* 294, 58–67. doi:10.1016/j.expneurol.2017.04.015.

60. Stewart, L. S., Persinger, M. A., Cortez, M. A., and Snead, O. C. (2007). Chronobiometry of behavioral activity in the Ts65Dn model of Down syndrome. *Behav Genet* 37, 388–398. doi:10.1007/s10519-006-9119-y.

61. Sun, X., Wu, Y., Chen, B., Zhang, Z., Zhou, W., Tong, Y., et al. (2011). Regulator of calcineurin 1 (RCAN1) facilitates neuronal apoptosis through caspase-3 activation. *J. Biol. Chem.* 286, 9049–9062. doi:10.1074/jbc.M110.177519.

62. Tranah, G. J., Blackwell, T., Stone, K. L., Ancoli-Israel, S., Paudel, M. L., Ensrud, K. E., et al. (2011). Circadian activity rhythms and risk of incident dementia and mild cognitive impairment in older women. *Ann Neurol.* 70, 722–732. doi:10.1002/ana.22468.

63. Van Egroo, M., Narbutas, J., Chylinski, D., Villar González, P., Maquet, P., Salmon, E., et al. (2019). Sleep–wake regulation and the hallmarks of the pathogenesis of Alzheimer's disease. *Sleep* 42. doi:10.1093/sleep/zsz017.

64. Vega, R. B., Rothermel, B. A., Weinheimer, C. J., Kovacs, A., Naseem, R. H., Bassel-Duby, R., et al. (2003). Dual roles of modulatory calcineurin-interacting protein 1 in cardiac hypertrophy. *Proceedings of the National Academy of Sciences* 100, 669–674. doi:10.1073/pnas.0237225100.

65. Vicari, S. (2006). Motor development and neuropsychological patterns in persons with Down syndrome. *Behav. Genet.* 36, 355–364. doi:10.1007/s10519-006-9057-8.

66. Wang, J. L., Lim, A. S., Chiang, W.-Y., Hsieh, W.-H., Lo, M.-T., Schneider, J. A., et al. (2015). Suprachiasmatic neuron numbers and rest-activity circadian rhythms in older humans: SCN and Rest-Activity Rhythms. *Ann Neurol.* 78, 317–322. doi:10.1002/ana.24432.

67. Wang, T., Liu, H., Wang, Y., Liu, C., and Sun, X. (2014). RCAN1 increases Aβ generation by promoting N-glycosylation via oligosaccharyltransferase. *Curr Alzheimer Res* 11, 332–339.

68. Weissová, K., Bartoš, A., Sládek, M., Nováková, M., and Sumová, A. (2016). Moderate changes in the circadian system of Alzheimer's disease patients detected in their home environment. *PLoS ONE* 11, e0146200. doi:10.1371/journal.pone.0146200.

69. Wisor, J. P., Edgar, D. M., Yesavage, J., Ryan, H. S., McCormick, C. M., Lapustea, N., et al. (2005). Sleep and circadian abnormalities in a transgenic mouse model of Alzheimer's disease: a role for cholinergic transmission. *Neuroscience* 131, 375–385. doi:10.1016/j.neuroscience.2004.11.018.

70. Wong, H., Levenga, J., Cain, P., Rothermel, B., Klann, E., and Hoeffer, C. (2015). RCAN1 overexpression promotes age-dependent mitochondrial dysregulation related to neurodegeneration in Alzheimer's disease. *Acta Neuropathol* 130, 829–843. doi:10.1007/s00401-015-1499-8.

71. Wu, Y., Deng, Y., Zhang, S., Luo, Y., Cai, F., Zhang, Z., et al. (2015). Amyloid-β precursor protein facilitates the regulator of calcineurin 1-mediated apoptosis by downregulating proteasome subunit α type-5 and proteasome subunit β type-7. *Neurobiology of Aging* 36, 169–177. doi:10.1016/j.neurobiolaging.2014.07.029.

72. Wu, Y., and Song, W. (2013). Regulation of RCAN1 translation and its role in oxidative stress-induced apoptosis. *The FASEB Journal* 27, 208–221. doi:10.1096/fj.12-213124.

73. Yin, M., Chen, Y., Zheng, H., Pu, T., Marshall, C., Wu, T., et al. (2017). Assessment of mouse cognitive and anxiety-like behaviors and hippocampal inflammation following a repeated and intermittent paradoxical sleep deprivation procedure. *Behav. Brain Res.* 321, 69–78. doi:10.1016/j.bbr.2016.12.034.

74. Zhao, H.-Y., Wu, H.-J., He, J.-L., Zhuang, J.-H., Liu, Z.-Y., Huang, L.-Q., et al. (2017). Chronic sleep restriction induces cognitive deficits and cortical beta-amyloid deposition in mice via BACE1-antisense activation. *CNS Neuroscience & Therapeutics* 23, 233–240. doi:10.1111/cns.12667.

Figures

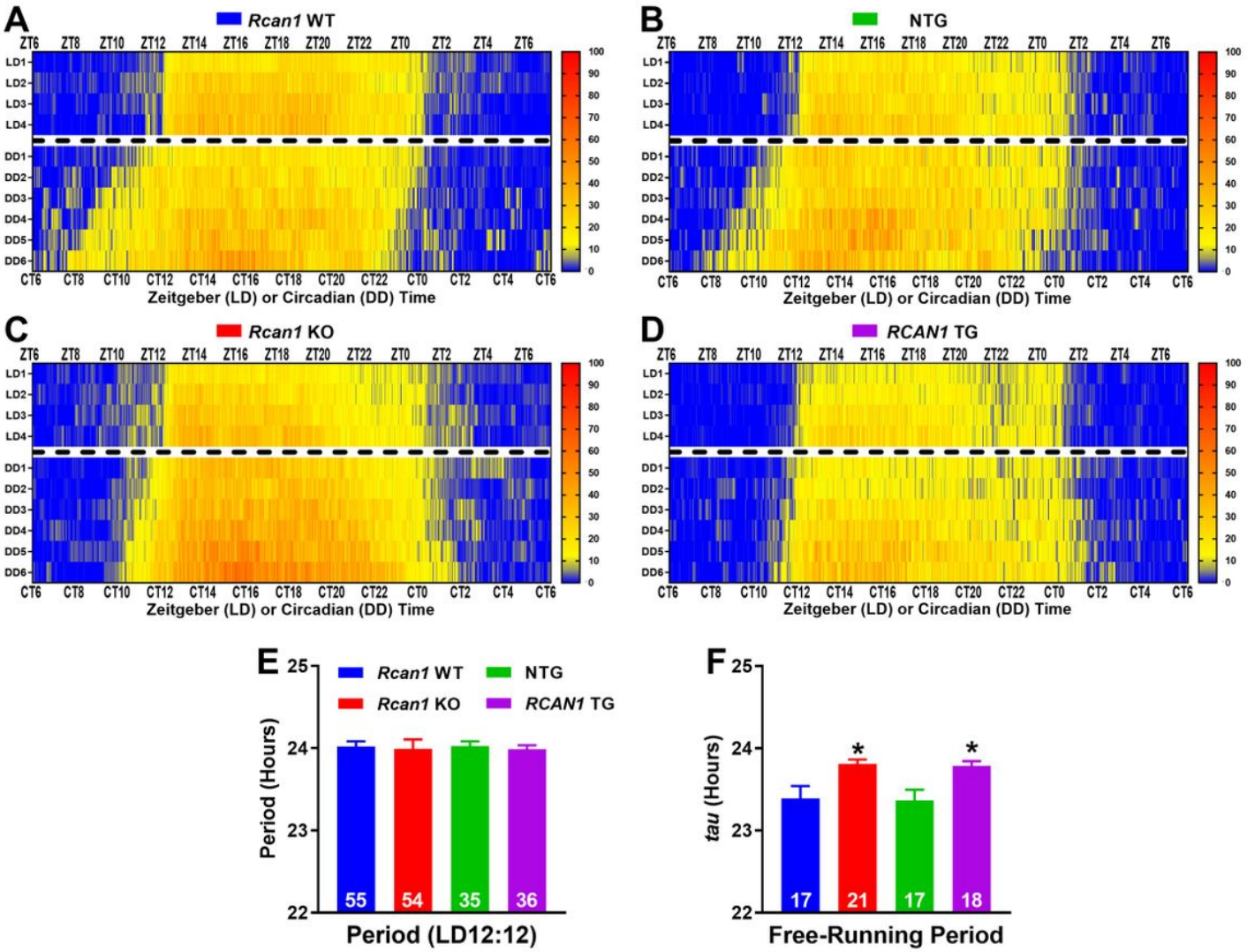

Figure 1

RCAN1 mediates the circadian periodicity but not the photic entrainment of wheel running. Heatmap-style actograms visualizing mean wheel revolution data for two distinct cohorts of mice tested in either LD12:12 conditions for a minimum of seven days (days -7 displayed) or DD conditions for a minimum of nine days (days 4-9 displayed) for (A) Rcan1 WT, (B) Rcan1 KO, (C) NTG, and (D) RCAN1 TG groups. (E) Light-entrained diurnal period length of wheel running rhythms in LD12:12. There were no group differences in light-entrained period length. (F) Circadian (free-running) period length of wheel running

rhythms in constant darkness. Young Rcan1 KO and RCAN1 TG mice have lengthened endogenous periods (tau) relative to young Rcan1 WT and NTG mice, respectively. All data are mean ± S.E.M. *p<0.05.

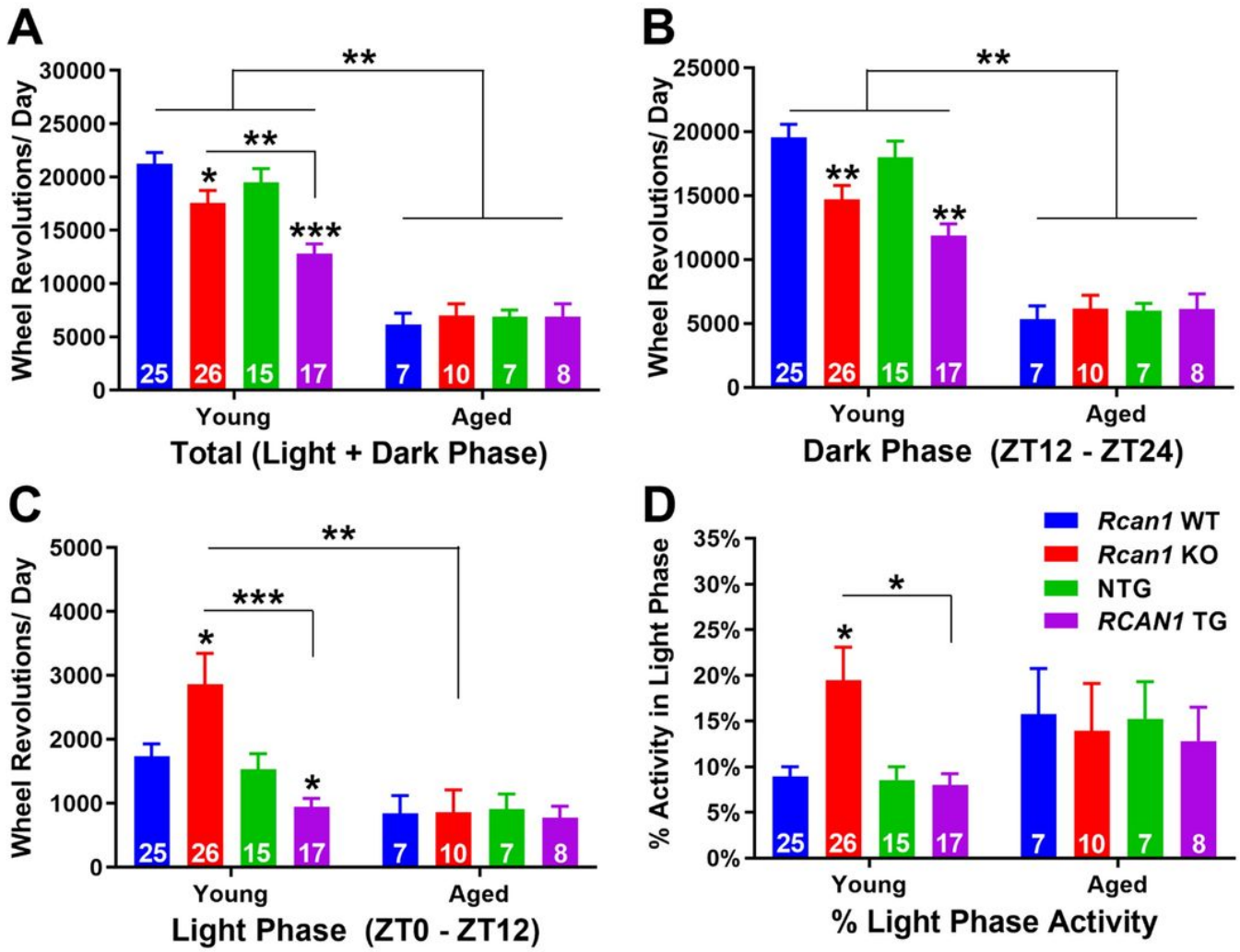

Figure 2

RCAN1 knockout and overexpression alter active and inactive phase wheel running patterns in light-entrained young but not aged mice. (A) Mean total daily wheel running of light-entrained young (left) and aged (right) mice. Young Rcan1 KO and RCAN1 TG mice exhibit reduced total daily wheel running relative to young RCAN1 WT and NTG controls, respectively. Compared with young mice, aged mice showed decreased total daily wheel running. (B) Mean daily dark phase (ZT12-ZT24) wheel running of light-entrained young (left) and aged (right) mice. Young Rcan1 KO and RCAN1 TG mice are hypoactive during the dark phase compared with young Rcan1 WT and NTG controls, respectively. Compared with young mice, aged mice showed decreased daily wheel running during the dark phase. (C) Mean daily light phase (ZT0-ZT12) wheel running of light-entrained young (left) and aged (right) mice. Young Rcan1 KO mice are hyperactive during the light phase compared with both young Rcan1 WT and RCAN1 TG mice as well as with aged Rcan1 KO mice. By contrast, young RCAN1 TG mice are hypoactive compared with young NTG controls. (D) Mean percentage of total daily wheel running during the light phase for light-entrained

young (left) and aged (right) mice. Young Rcan1 KO mice have an increased percentage of total daily activity occurring during the light phase compared with young Rcan1 WT and RCAN1 TG mice. All data are mean ± S.E.M. *p<0.05; **p<0.01; ***p<0.001.

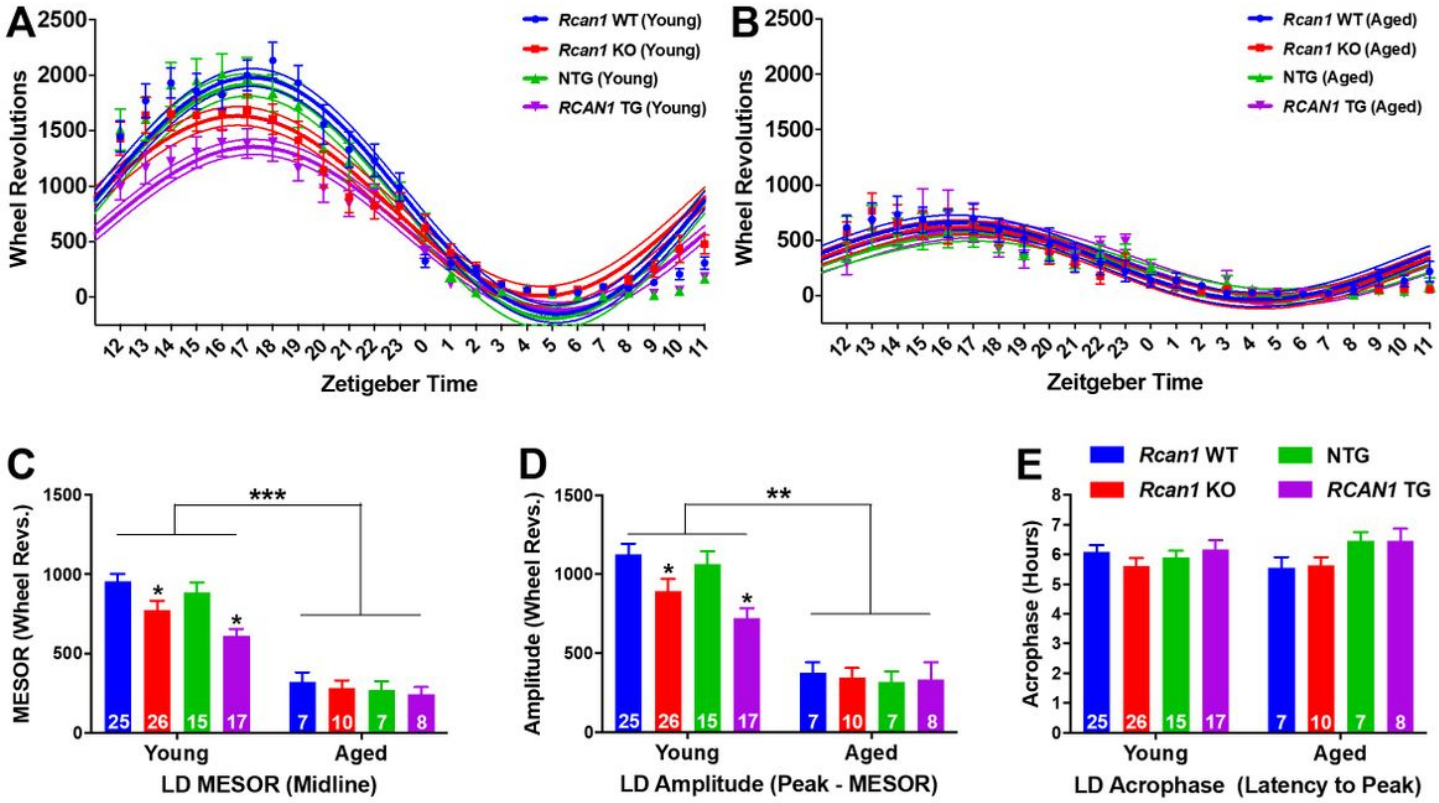

Figure 3

RCAN1 knockout and overexpression similarly attenuate the light-entrained diurnal rhythmicity of wheel running in young but not aged mice. Plots of average daily wheel revolutions collapsed into hourly bins (floating points depicting mean ± S.E.M) with superimposed single-harmonic regression curve fits (mean ± 95% CI bands) for (A) young and (B) aged mice. (C) Mean daily MESOR estimates for wheel running rhythms of light-entrained young (left) and aged (right) mice. Young Rcan1 KO and RCAN1 TG mice have decreased MESOR estimates versus young Rcan1 WT and NTG mice, respectively. Aged Rcan1 WT and NTG mice showed reduced MESOR estimates relative to young Rcan1 WT and NTG mice, respectively. (D) Mean daily amplitude estimates for wheel running rhythms of light-entrained young (left) and aged (right) mice. Young Rcan1 KO and RCAN1 TG mice have reduced amplitude estimates compared with young Rcan1 WT and NTG mice, respectively. Aged Rcan1 WT and NTG mice showed decreased amplitude estimates relative to young Rcan1 WT and NTG mice, respectively. (E) Mean daily acrophase estimates for wheel running rhythms of light-entrained young adult (left) and aged (right) mice. There were no group differences in acrophase estimates. All data are mean ± S.E.M. **p<0.01; ***p<0.001.

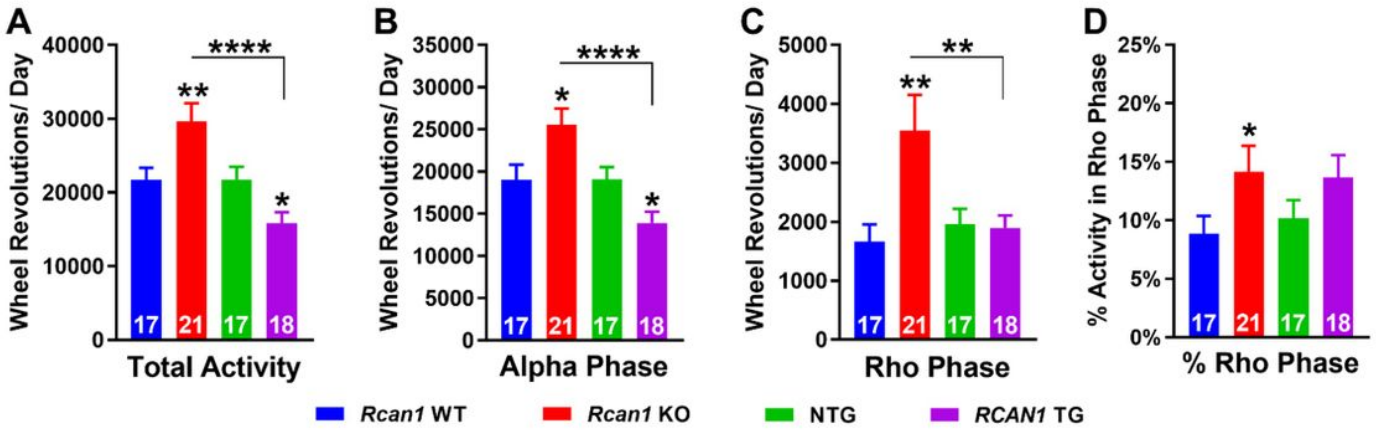

Figure 4

RCAN1 knockout and overexpression bidirectionally perturb wheel running patterns of free-running young mice. (A) Mean total (CT0-CT24) daily wheel running of free-running young mice. Rcan1 KO mice exhibit increased total daily wheel running compared with Rcan1 WT and RCAN1 TG mice, while RCAN1 TG mice displayed decreased total daily wheel running compared with NTG mice. (B) Mean daily alpha (active) phase wheel running of free-running young mice in DD. Rcan1 KO mice show increased daily wheel running in the alpha phase compared with Rcan1 WT and RCAN1 TG mice, while RCAN1 TG mice show decreased daily wheel running in the alpha phase relative to NTG mice. (C) Mean daily rho (inactive) phase wheel running of free-running young mice in DD. Rcan1 KO mice exhibit elevated daily wheel running during the rho phase compared with Rcan1 WT and RCAN1 TG mice. (D) Mean percentage of total daily wheel running during the rho phase for free-running young mice. Rcan1 KO mice display an increased percentage of total daily wheel running in the rho phase compared with Rcan1 WT mice, while RCAN1 TG mice trended toward an increased percentage of total daily activity in the rho phase compared to NTG mice. All data are mean ± S.E.M. *p<0.05; **p<0.01; ****p<0.0001.

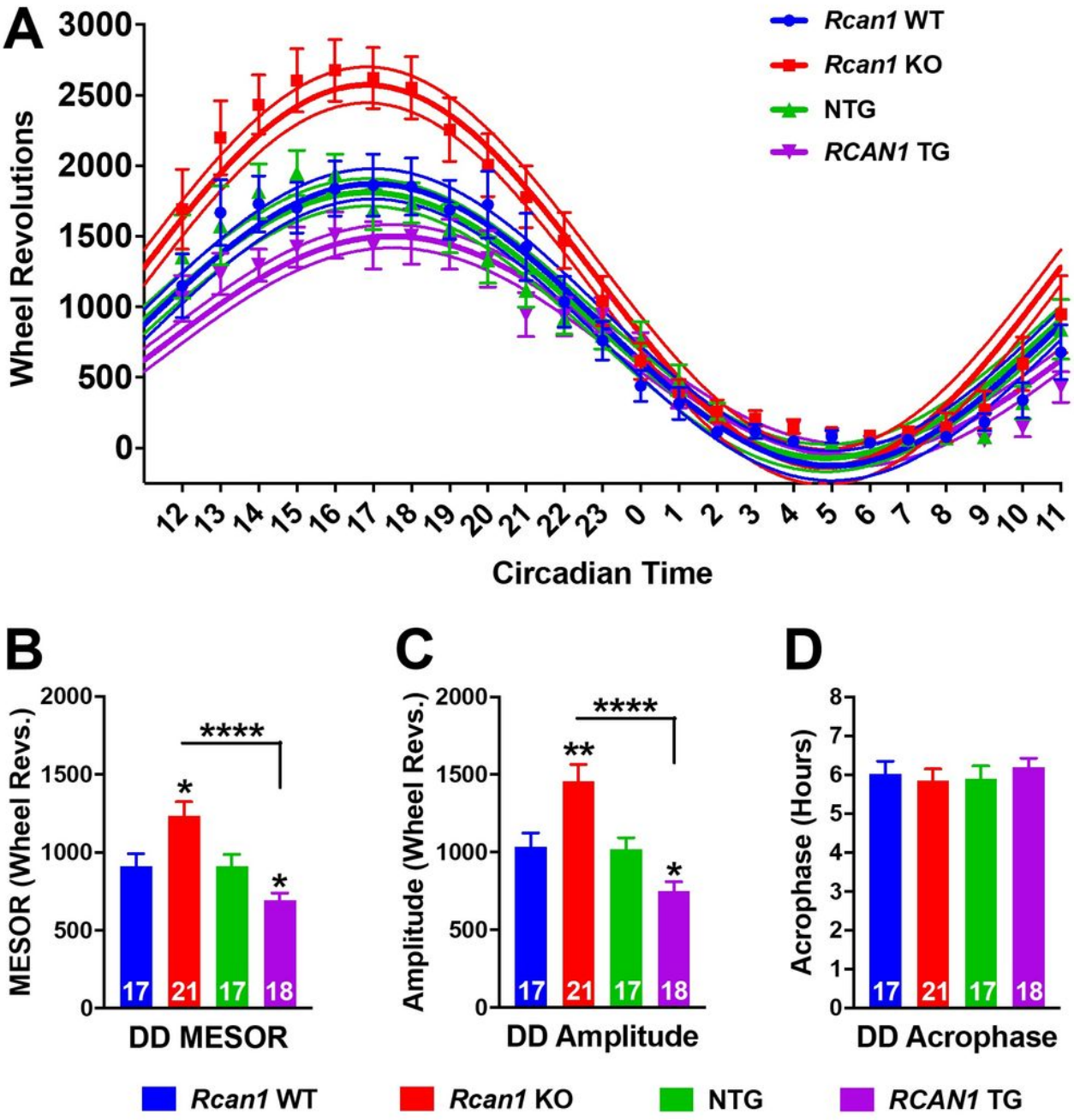

Figure 5

RCAN1 knockout and overexpression elicit divergent alterations in the circadian rhythmicity of wheel running in young mice. (A) Plot of average daily wheel revolutions collapsed into hourly bins (floating points depicting mean ± S.E.M) with superimposed single-harmonic regression curve fits (mean ± 95% CI bands) for free-running young mice. (B) Mean daily MESOR estimates for wheel running rhythms of free-running young mice. Rcan1 KO mice exhibit increased daily MESOR estimates compared with Rcan1 WT

and RCAN1 TG mice, while RCAN1 TG mice display decreased daily MESOR estimates relative to NTG mice. (C) Mean daily amplitude estimates for wheel running rhythms of free-running young mice. Rcan1 KO mice exhibit increased daily amplitude estimates compared with Rcan1 WT and RCAN1 TG mice, while RCAN1 TG mice display decreased daily amplitude estimates compared with NTG mice. (D) Mean daily acrophase estimates for wheel running rhythms of free-running young mice. There were no group differences in acrophase estimates. All data are mean ± S.E.M. *p<0.05; **p<0.01; ****p<0.0001.

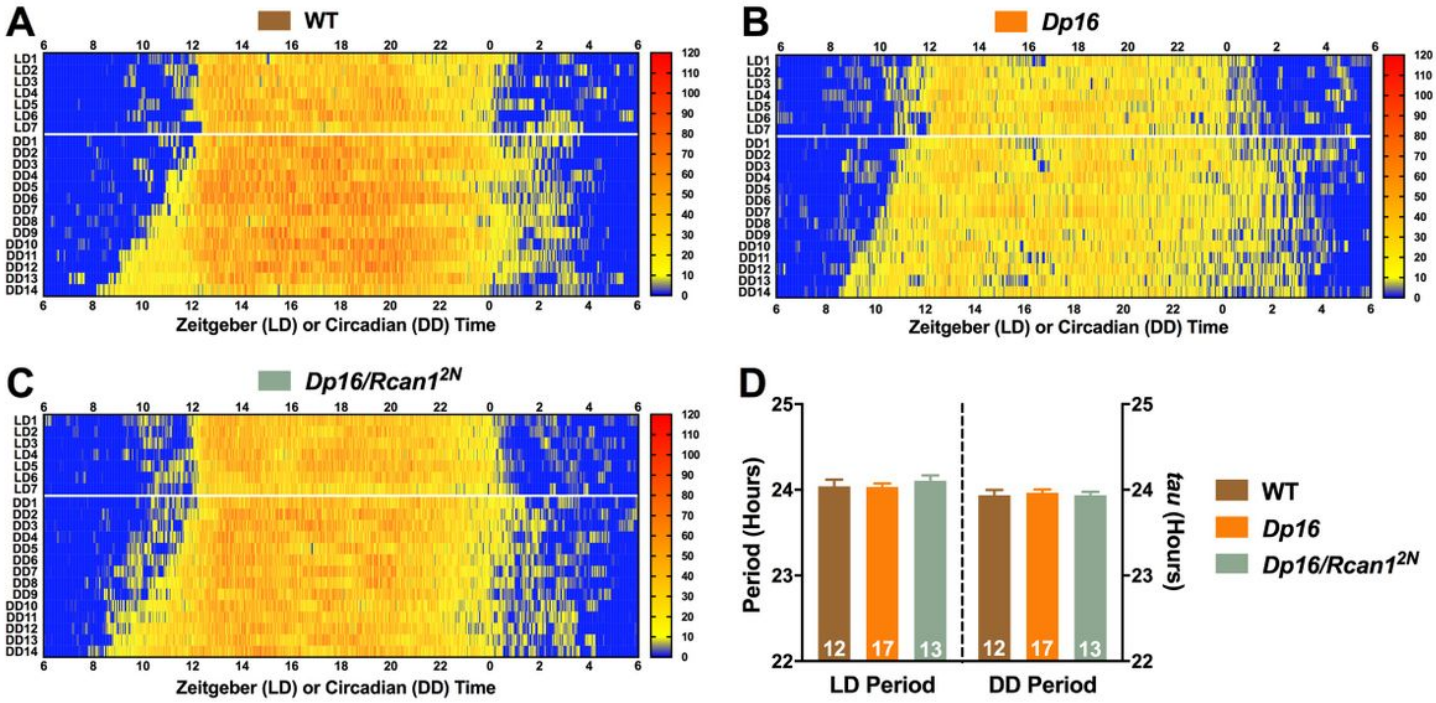

Figure 6

Photic entrainment and circadian periodicity of wheel running are unaltered in young Dp16 mice independent of Rcan1 copy number. Heatmap-style actograms visualizing mean wheel revolution data for (A) WT, (B) Dp16, and (C) Dp16/Rcan12N mice tested in LD12:12 conditions for fourteen days (days 8-14 displayed) and immediately transferred to and tested in DD conditions for fourteen days (days 1-14 displayed). (D) Mean wheel running period lengths for light-entrained (left) and free-running (right) young mice. No group differences in either light-entrained or free-running (endogenous) period length were detected. All data are mean ± S.E.M.

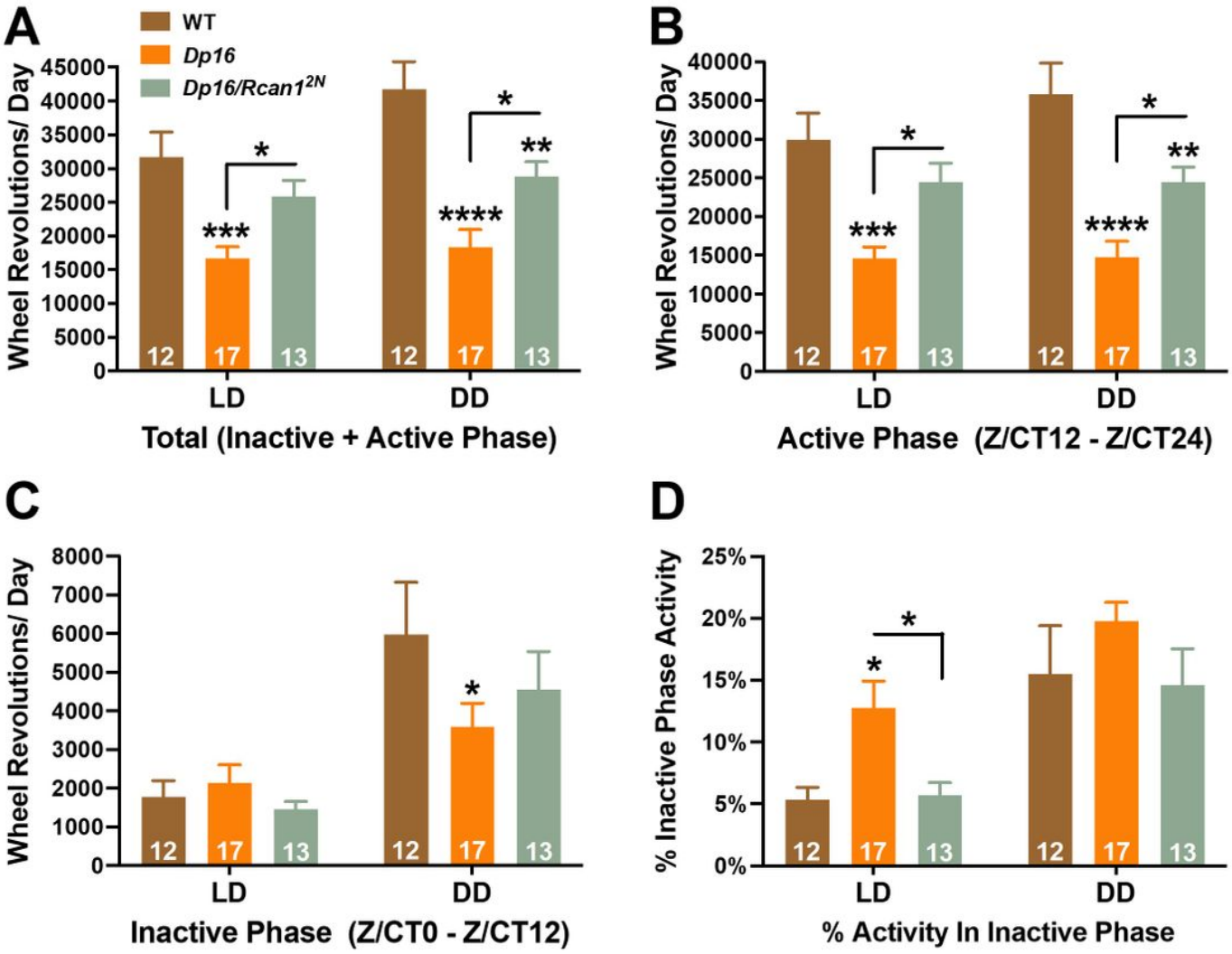

Figure 7

Altered wheel running patterns in light-entrained and free-running young Dp16 mice are partially normalized by restoration of Rcan1 to two copies. (A) Mean total daily wheel running of light-entrained (left) and free-running (right) young mice. Light-entrained young Dp16 mice exhibited decreased total daily wheel running compared with WT and Dp16/Rcan12N mice. Free-running young Dp16 mice displayed reduced total daily wheel running relative to both WT and Dp16/Rcan12N mice, and free-running young Dp16/Rcan12N mice exhibited decreased total daily wheel running versus WT mice. (B) Mean daily active phase wheel running of light-entrained (left) and free-running (right) young mice. Light-entrained young Dp16 mice exhibited decreased active phase wheel running compared with WT and Dp16/Rcan12N mice. Free-running young Dp16 mice displayed reduced active phase wheel running relative to both WT and Dp16/Rcan12N mice, and free-running young Dp16/Rcan12N mice exhibited decreased active phase wheel running versus WT mice. (C) Mean daily inactive phase wheel running of light-entrained (left) and free-running (right) young mice. No group differences were detected for inactive

phase wheel running among light-entrained mice. However, free-running young Dp16 mice displayed reduced inactive phase wheel running relative to WT mice. (D) Mean percentage of total daily wheel running during the inactive phase for light-entrained (left) and free-running (right) young mice. Light-entrained young Dp16 mice exhibited increased percent inactive phase wheel running compared with WT and Dp16/Rcan12N mice. No group differences were detected for percent inactive phase wheel running among free-running mice. All data are mean ± S.E.M. *p<0.05; **p<0.01; ***p<0.001; ****p<0.0001.

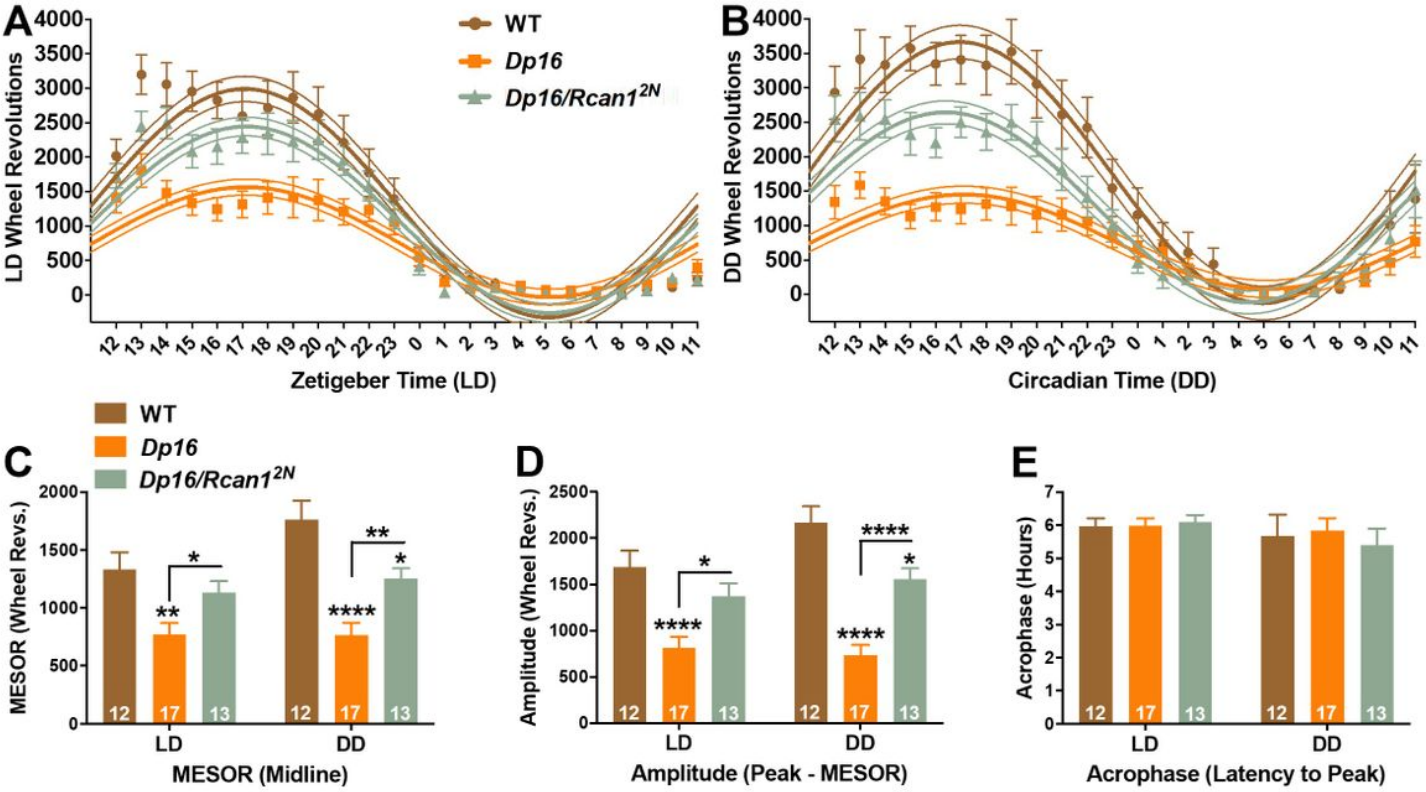

Figure 8

Light-entrained diurnal and circadian wheel running rhythms are diminished in young Dp16 mice and are partially normalized by restoration of Rcan1 to two copies. Plots of average daily wheel revolutions collapsed into hourly bins (floating points depicting mean ± S.E.M) with superimposed single-harmonic regression curve fits (mean ± 95% CI bands) for (A) light-entrained and (B) free-running young mice. (C) Mean daily MESOR estimates for wheel running rhythms of light-entrained (left) and free-running (right) young mice. Light-entrained young Dp16 mice exhibited decreased MESOR estimates compared with WT and Dp16/Rcan12N mice. Free-running young Dp16 mice displayed reduced MESOR estimates relative to both WT and Dp16/Rcan12N mice, and free-running young Dp16/Rcan12N mice exhibited decreased MESOR estimates versus WT mice. (D) Mean daily amplitude estimates for wheel running rhythms of light-entrained (left) and free-running (right) young mice. Light-entrained young Dp16 mice exhibited decreased amplitude estimates compared to WT and Dp16/Rcan12N mice. Free-running young Dp16

mice displayed reduced amplitude estimates relative to both WT and Dp16/Rcan12N mice, and free-running young Dp16/Rcan12N mice exhibited decreased amplitude estimates versus WT mice. (E) Mean daily acrophase estimates for wheel running rhythms of light-entrained (left) and free-running (right) young mice. There were no group differences in acrophase estimates. All data are mean ± S.E.M. *p<0.05; **p<0.01; ****p<0.0001.

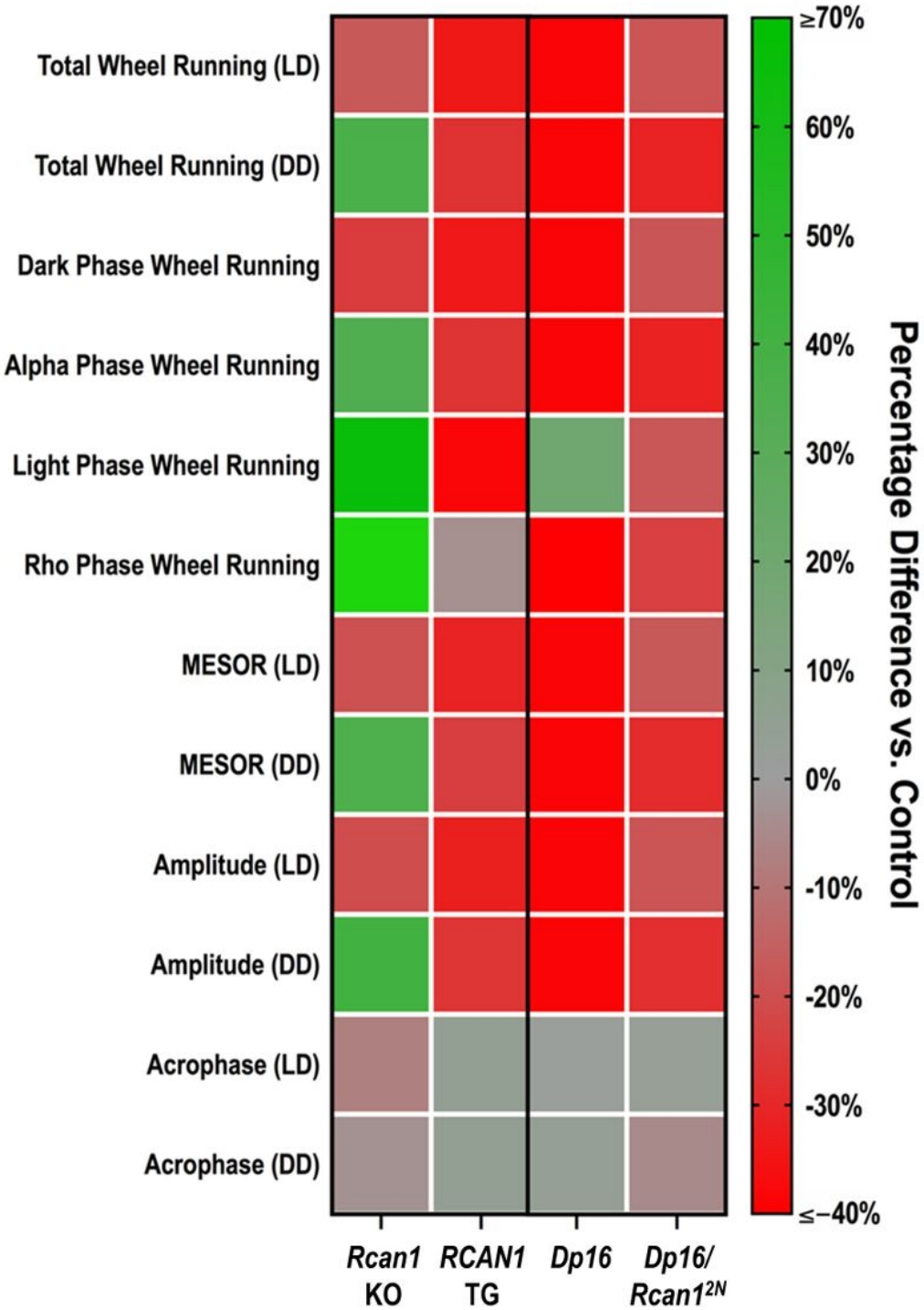

Figure 9

Survey of wheel running phenotypes in young Rcan1 KO, RCAN1 TG, Dp16, and Rcan1 dosage-corrected Dp16 mice. Dual-gradient heatmap depicting the percentage differences of young Rcan1 KO and Rcan1 TG mice relative to young Rcan1 WT and NTG control mice, respectively (left horizontal axis) as well as young Dp16 and Dp16/Rcan12N mice relative to young WT control mice (right horizontal axis) for measures of wheel running patterns and rhythms in light-entrained (LD) and free-running (DD) conditions (vertical axis). A percentage difference of zero indicates no difference (depicted in gray) relative to the corresponding control group, whereas percentage differences of ≤-40% and ≥70% indicate a 40% or greater decrease (depicted in red) and a 70% or greater increase (depicted in green), respectively, relative to the corresponding control group.

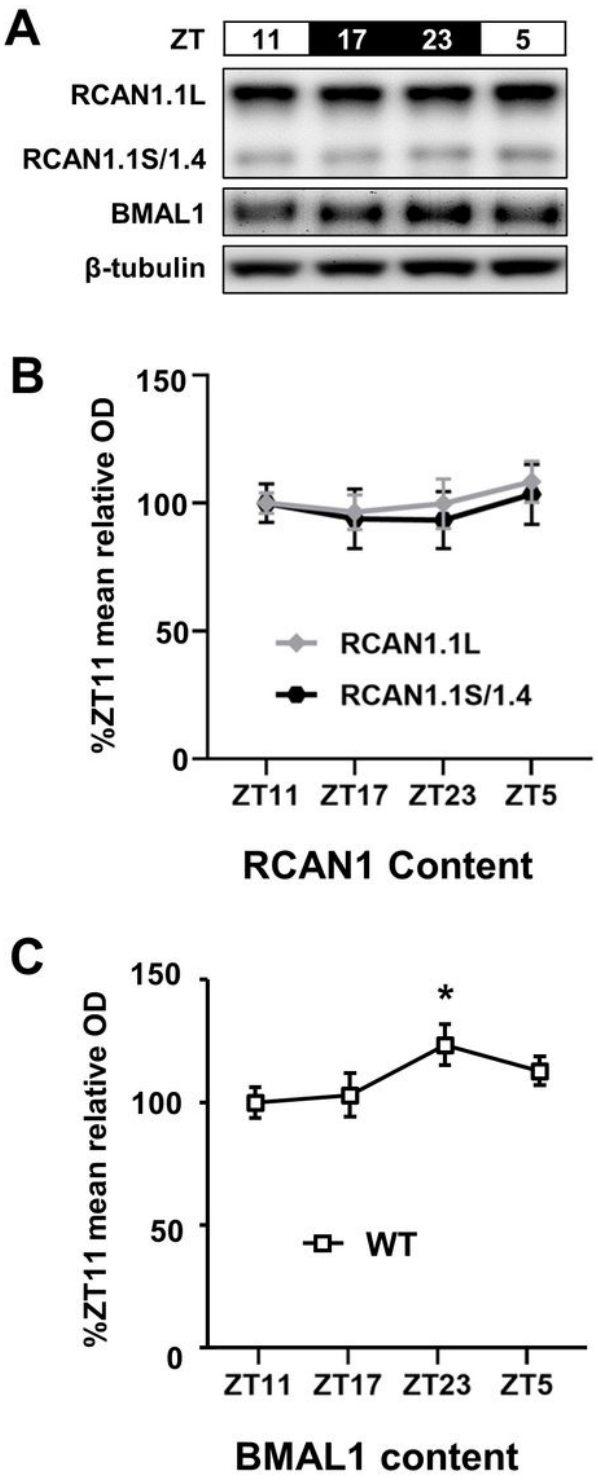

Figure 10

Hippocampal RCAN1 expression is normally arrhythmic in young mice. (A) Representative Western blot images of RCAN1 and BMAL1 in the hippocampi of Rcan1 WT adult mice (3-6 months old) at ZT11, ZT17, ZT23, and ZT5. RCAN1 isoforms: RCAN1.1L (~38 kDa), RCAN1.1S (~28 kDa), and RCAN1.4 (~28 kDa). β-tubulin, loading control. (B) Densitometric measurements of RCAN1 isoform abundance normalized to β-tubulin levels are displayed as percentages of the mean relative optical density (OD) in

ZT11 hippocampi. There were no temporal variations in RCAN1.1L and RCAN1.1S/1.4 levels for any time point assessed. (C) Densitometric measurements of BMAL1 abundance normalized to ¬β-tubulin levels are displayed as percentages of the mean relative OD in ZT11 hippocampi. BMAL1 levels were significantly elevated at ZT23 compared with ZT11. All data are mean ± S.E.M. *p<0.05.